# Myd88 initiates early innate responses and promotes CD4 T cells during coronavirus encephalomyelitis

Niranjan Butchi[#§], Parul Kapil[1&§], Shweta Puntambekar[1], Stephen A. Stohlman[1], David R. Hinton[2], Cornelia C. Bergmann[1]*

[1]Department of Neurosciences, NC-30, Lerner Research Institute, Cleveland Clinic Foundation, 9500 Euclid Avenue, Cleveland, OH 44195, USA. [2]Department of Pathology, Keck School of Medicine, University of Southern California, Los Angeles, CA 90033, USA.

[#]deceased July 17, 2013.

[&]Current address: DETTD, Center for Biologics Evaluation & Research (CBER), US Food and Drug Administration, 10903 New Hampshire Avenue, Silver Spring, MD 20993, USA.

**Running Title: Myd88 mediated protection during viral encephalomyelitis**

**Word count:** Abstract (244), Importance (148), Introduction (798), Materials and Methods (1318), Results (2865), Discussion (1551), Figures legends (895), References (2188); Total word count: (10222)

**§ authors contributed equally**

***Corresponding author:**
Cornelia C. Bergmann
Lerner Research Institute
Cleveland Clinic Foundation
9500 Euclid Avenue
Cleveland, OH 44195
Phone (001) 216-444-5922
Fax (001) 216-444-7927
Email: bergmac@ccf.org

**Key Words:** coronavirus, central nervous system, Myd88, CD4 T cells, IFNγ

**Abstract**

Myd88 signaling is critical to control numerous central nervous system (CNS) infections by promoting both innate and adaptive immune responses. Nevertheless, the extent to which Myd88 regulates type I IFN versus proinflammatory factors and T cell function, as well as anatomical site of action varies extensively with the pathogen. CNS infection by neurotropic coronavirus with confined replication in brain and spinal cord induces protective IFNα/β via Myd88 independent activation of melanoma differentiation-associated gene 5 (MDA5). However, a contribution of Myd88 dependent signals to CNS pathogenesis has not been assessed. Infected Myd88$^{-/-}$ mice failed to control virus, exhibited enhanced clinical disease coincident with increased demyelination, and succumbed to infection within three weeks. Induction of IFNα/β, as well as proinflammatory cytokines and chemokines was impaired early during infection. However, defects in both IFNα/β and select proinflammatory factors were rapidly overcome prior to T cell recruitment. Myd88 deficiency also specifically blunted myeloid and CD4 T cell recruitment into the CNS without affecting CD8 T cells. Moreover, CD4 T cells, but not CD8 T cells, were impaired in IFNγ production. Ineffective virus control indeed correlated most prominently with reduced anti-viral IFNγ in the CNS of Myd88$^{-/-}$ mice. The results demonstrate a crucial role for Myd88 both in early induction of innate responses during coronavirus induced encephalomyelitis and in specifically promoting protective CD4 T cell activation. In the absence of these responses, functional CD8 T cells are insufficient to control viral spread within the CNS resulting in severe demyelination.

52

53 **Importance**

54 During central nervous system (CNS) infections signaling through the adaptor protein Myd88
55 promotes both innate and adaptive immune responses. The extent to which Myd88 regulates
56 antiviral type I IFN, pro inflammatory factors, adaptive immunity and pathology is pathogen
57 dependent. These results reveal that Myd88 protects from lethal neurotropic coronavirus induced
58 encephalomyelitis by accelerating, but not enhancing, IFNα/β as well as promoting peripheral
59 activation and CNS accumulation of virus specific CD4 T cells secreting IFNγ. By controlling
60 both early innate responses and CD4 T cell mediated antiviral IFNγ, Myd88 signaling limits
61 initial viral dissemination and is vital for T cell mediated control of viral load. Uncontrolled viral
62 replication in the absence of Myd88 leads to severe demyelination and pathology despite overall
63 reduced inflammatory responses. These data support a vital role of Myd88 signaling in protective
64 antimicrobial function in the CNS by promoting proinflammatory mediators and T cell mediated
65 IFNγ production.

66

## Introduction

Rapid anti-viral responses are initiated by a diverse array of pattern recognition receptors (PRRs) responding to pathogen associated molecular patterns. These include membrane bound Toll like receptors (TLRs) at the cell surface and endocytic compartments as well as cytoplasmic RNA helicases RIG-I and MDA5 (51, 52). Both structural components and replication cycle of the virus as well as the respective identity of the activated PPRs dictate the magnitude and selectivity of the response. The viral structures and specific PRRs triggering innate responses, especially type I IFN, have been identified for numerous viruses (8, 52). However, analysis of distinct cell types in combination with *in vivo* studies are revealing a more complex picture in which the innate host response is coordinated by several pathways involving multiple PRRs (8, 16, 50, 52). Efficient regulation of these pathways is especially crucial within the central nervous system (CNS), where innate activation is not only vital to limit viral spread via type I IFN, but also to facilitate leukocyte recruitment and expression of their effector functions via induction of proinflammatory mediators. Nevertheless, the highly restricted and cell type specific magnitude and diversity of PRR expression (8, 10, 21, 35) suggests tight regulation to initiate inflammation, while avoiding irrelevant or excessive activation leading to bystander tissue damage.

The unifying factor required to transmit signals from most TLRs, excluding TLR3, is the adaptor protein Myd88, which also transmits signals through the IL1 and IL18 receptors (51, 52). Myd88 is critical for upregulation of proinflammatory genes and recruitment of leukocytes during numerous CNS infections and plays a protective role during Vesicular stomatitis virus (VSV) (25), West Nile virus (WNV) (50), Herpes simplex virus-1 (HSV-1) (30), Herpes simplex virus-1 (HSV-2) (48) and *toxoplasma gondii* infection (53). However, the underlying mechanisms are only partially defined and differ among distinct infections, and even virus



Journal of Virology

strains. For example, both HSV-1 and HSV-2 activate TLR2 and TLR9 *in vitro* via a virus surface component and virus DNA, respectively. However, while infected Myd88$^{-/-}$ mice succumb to HSV-1, TLR2$^{-/-}$ mice survive similar to wildtype (wt) mice (30), suggesting TLR2 is redundant *in vivo*. By contrast, studies with a distinct HSV-1 strain indicated TLR2 signaling mediates enhanced encephalitis and mortality (23). Peripheral infection with HSV-2 also demonstrated increased viral loads in brain, but not liver, of mice deficient in Myd88 or dually deficient in both TLR2 and TLR9; however, deficiency in either TLR alone did not alter viral load, despite affecting cytokine and chemokine profiles (48). Unlike HSV, WNV primarily activates innate responses within the CNS through MDA5 and RIG-I via the MAVS adapter (15, 49). Despite this Myd88 independent pathway, WNV infection of TLR7$^{-/-}$ as well as Myd88$^{-/-}$ mice revealed impaired viral control and leukocyte migration into the CNS associated with peripheral defects in IL23, but not IFNα/β, IL6 or TNF (54). In a separate study, WNV infected Myd88$^{-/-}$ mice also exhibited increased mortality coincident with enhanced viral spread specifically within the CNS, but not peripheral organs. In this case uncontrolled virus was associated with reduced proinflammatory responses and leukocyte recruitment into the CNS, yet no defects in peripheral T cell activation, CNS IFNα/β, or CNS virus specific T cell responses were detected (50).

Similar to WNV infection, PRR dependent IFNα/β production is vital to prevent peripheral dissemination of mouse hepatitis virus (MHV) strain A59, as well as spread of the glia tropic JHMV strain within the CNS (7, 9, 19). While peripheral MHV infection is sensed via Myd88 dependent TLR7 in plasmacytoid dendritic cells (9), MDA5 is the primary sensor inducing IFNα/β in microglia/macrophages (43). A contribution of Myd88 signaling during encephalomyelitis mediated by infection with gliatropic JHMV, which is associated with

113 minimal if any productive replication in draining lymph node dendritic cells (60), has not been
114 assessed. Following JHMV infection IFNα/β prevents neuronal infection and restrains viral
115 spread within the CNS prior to emergence of adaptive immunity (19). T cells subsequently
116 control CNS viral replication within two weeks via IFNγ and perforin mediated mechanisms, but
117 are insufficient to provide sterile immunity, resulting in viral RNA persistence (3, 27, 34). Given
118 the crucial roles of both innate and adaptive components to antiviral protection within the CNS,
119 the current studies assessed the role of Myd88 in regulating inflammation and antiviral activity
120 during JHMV induced encephalomyelitis.

121 Infection of Myd88$^{-/-}$ mice revealed that early innate responses were transiently impaired,
122 but rapidly overcome by Myd88 independent signals. Uncontrolled viral replication correlated
123 with significantly diminished IFNγ and IFNγ dependent MHC upregulation supporting impaired
124 anti-viral T cell effector function *in vivo*. Moreover, myeloid and CD4 T cell, but not CD8 T cell
125 recruitment to the CNS were significantly blunted. The results demonstrate a crucial biphasic
126 role for Myd88 in supporting a rapidly induced innate response early during coronavirus
127 encephalomyelitis and subsequently promoting protective CD4 T cell functions during the
128 adaptive phase.
129

## Materials and Methods

### Mice, viruses and infections

C57BL/6 mice were purchased from the National Cancer Institute (Frederick, MD). Homozygous Myd88$^{-/-}$ mice (B6.129P2(SJL)-*Myd88*$^{tm1Defr}$/J, stock number 008888, Jackson Laboratories, Bar Harbor, ME) on the C57BL/6 background were kindly provided by Dr. Robert Fairchild (Cleveland Clinic, Cleveland, OH) and bred locally. Mice were housed under pathogen free conditions in an accredited facility at the Cleveland Clinic Lerner Research Institute. All animal procedures were performed in compliance with protocols approved by the Cleveland Clinic Institutional Animal Care and Use Committee (PHS assurance number: A3047-01). Mice at 6-7 weeks of age were infected intracranially in the left hemisphere with 1000 PFU of the sublethal, gliatropic, monoclonal antibody (mAb) derived variant of JHMV, designated 2.2v-1 (13), in 30 µl endotoxin-free Dulbecco's phosphate-buffered saline (PBS). Clinical disease severity was graded daily using the following scale: 0, healthy; 1, ruffled fur/hunched back; 2, inability to turn upright/partial hind limb paralysis; 3, complete hind limb paralysis; 4, moribund or dead (22, 39, 44). Infectious virus in cell free supernatants was determined by plaque assay on DBT astrocytoma monolayers as described (13). Briefly, individual brains were homogenized in 4 ml Dulbecco's PBS using chilled Tenbroeck glass homogenizers. Homogenates were clarified by centrifugation at 400 x g for 7 min at 4$^{o}$C, and supernatants stored at -70$^{o}$C until use for plaque assay.

### RNA extraction, reverse transcription, and gene expression analysis

RNA was extracted using TRIzol reagent (Invitrogen, Carlsbad, CA) according to the manufacturer's instructions and subjected to real time PCR analysis as described (7, 22, 39). In

brief, snap frozen tissues were dissociated with TRIzol in a Tissuelyser II (Qiagen, Valencia, CA), treated with chloroform, and RNA precipitated with isopropyl alcohol. Following washing with 75% ethanol, RNA was resuspended in RNase-free water (Gibco/Invitrogen, Grand Island, NY) and treated with DNase I using a DNA Free™ kit (Ambion, Austin, TX) for 30 min at 37°C following the manufacturer's instructions. 2 µg RNA was converted to cDNA using the Moloney murine leukemia virus reverse transcriptase (Invitrogen) in buffer containing 10 mM deoxynucleoside triphosphate mix, 250 ng random hexamer primers, and oligo(dT) (1:1 ratio) (Invitrogen). cDNA samples were diluted ten-fold in RNase-free water before analysis by quantitative real-time PCR using either SYBR green master mix (Applied Biosystems, Foster City, CA) or Taqman technology as described (7, 22). The primer sequences for SYBR green PCR analysis are as follows: (F, forward; R, reverse): *Gapdh*, F, 5'-CATGGCCTTCCGTGTTCCTA-3' and R, 5'-ATGCCTGCTTCACCACCTTCT-3'; *Il6*, F, 5'-ACACATGTTCTCTGGGAAATCGT-3' and R, 5'-AAGTGCATCAT CGTTGTTCATACA-3'; *Il10*, F, 5'- TTTGAATTCCCTGGGTGAGAA-3' and R, 5'-GCTCCACTGCCTTGCTCTTATT-3'; *Il21*, F, 5'- GGACAGTATAGACGCTCACGAATG -3' and R, 5'- CGTATCGTACTTCTCCACTTGCA-3'; *Tnf*, F, 5′-GCCACCACGCTCTTCTGTCT-3′, and R, 5′-GGTCTGGGCCATAGAACTGATG-3′; *Nos2*, F, 5'-CCTGGTA CGGGCATTGCT-3' and R, 5'-CATGCGG CCTCCTTTGAG-3'; *Ccl3*, F, 5'- -3' and 5'- -3'; *Ccl5*, F, 5'-GCAAGTGCTCCAATCTTGCA-3' and 5'-CTTCTCTGGGTTGGCACACA-3'; *Cxcl10*, F, 5'-GACGGTCCGCTGCAACTG-3' and R, 5'-GCTTCCCTATGGCCCTCATT-3'; *Cxcl13*, F, 5'- -3' and 5'- -3'; and *viral nucleocapsid (N) protein encoding RNA*, F, 5'-GCCAAATAATC GCGCTAGAA-3' and R, 5'-CCGA GCTTAGCCAAAACAAG-3'. All samples were run in duplicate on a 96-well plate using a

7500 Fast Real Time PCR system (Applied Biosystems) with an automatic set baseline and a manual set critical threshold (CT) at which the fluorescent signal becomes higher than all of the PCR pairs. Dissociation curves were used to confirm amplification of a single product for each primer pair per sample. Expression levels of *Gapdh, Cxcl1, Ccl2, Ifnα4, Ifnα5, Ifnβ1, Ifnγ, Ifit1, Ifit2, Isg15,* and *Il1β* were determined using TaqMan primer and probe sets, and 2x universal TaqMan fast master mix (Applied Biosystems). Data were calculated relative to the housekeeping gene *Gapdh* using the following formula: $2^{[CT(GAPDH) - CT(Target\ Gene)]}$ X 1000 .

**Cell isolation, flow cytometry and intracellular cytokine staining**

Cells for flow cytometric analysis were isolated from brains as described (7, 22, 44). Briefly, mice were perfused with PBS and brains homogenized in 4 ml of Dulbecco's PBS (pH 7.4) using Tenbroeck tissue homogenizers. Following centrifugation at 400 x g for 7 min, cell pellets were resuspended in RPMI containing 25 mM HEPES (pH 7.2), adjusted to 30% Percoll (Pharmacia, Uppsala, Sweden) and underlayed with 1ml of 70% Percoll. Following centrifugation at 800 x g for 30 min at 4°C, cells were recovered from the 30%/70% interface, washed with RPMI and suspended in FACS buffer (0.5% bovine serum albumin in Dulbecco's PBS). Fcγ receptors were blocked with 1% mouse serum and 1% rat anti-mouse CD16/CD32 (clone 2.4G2; BD Biosciences, San Jose, CA) mAb for 20 min. Specific cell types were identified by staining with fluorescein isothiocyanin (FITC)-, phycoerythrin (PE)-, peridinin chlorophyll protein (PerCP)-, or allophycocyanin (APC)-conjugated mAb for 30 min on ice in FACS buffer. Expression of surface markers was characterized with mAb (all from BD Biosciences except when indicated) specific for CD45 (clone Ly-5), CD4 (clone GK1.5), CD8 (clone 53-6.7), F4/80 (Serotec, Raleigh, NC), Ly-6G (clone 1A8), and MHC class II (clone

2G9). Virus specific CD8 T cells were identified using H-2D$^b$/S510 MHC class I tetramers as described previously (19, 22, 39, 61). Samples were analyzed using a FACS Calibur flow cytometer (BD Biosciences) and Flow-jo 7 software (Treestar, Inc., Ashland, OR).

IFNγ production by T cells was measured by intracellular flow cytometry following stimulation of 5x10$^5$ CNS derived cells with 3x10$^5$ EL4 or CHB3 feeder cells with or without virus specific class I or class II restricted peptide for 5h as described (22, 61). Briefly, CD8 and CD4 T cells were stimulated with 1μM S510 or 10 μM M133, respectively, in a total volume of 200μl of RPMI supplemented with 10% fetal calf serum for 5 h at 37$^o$ C with Golgi Stop (BD Biosciences). Following surface staining for CD8, CD4 and CD45, cells were fixed and permeabilized using the Cytofix/Cytoperm kit (BD Biosciences) according to the manufacturer's protocol. Intracellular cytokines were detected using FITC conjugated anti-IFNγ mAb. Cells were analyzed by flow cytometry as described above.

**Immunohistochemistry**

Brains divided along the mid-sagittal plane from PBS-perfused mice were fixed with 10% $Zn^+$ formalin and embedded in paraffin. Spinal cords were divided into 6 equivalent length segments from cervical to lumbar and embedded in paraffin together allowing cross sections from individual mice to be examined at each of the 6 levels. Sections were stained with either hematoxylin and eosin (H&E) or luxol fast blue (LFB) as described (20, 38, 40). Cells containing the viral nucleocapsid (N) protein were identified by immunoperoxidase staining using mAb J.3.3 as primary antibody, biotinylated horse anti-mouse as secondary antibody, and streptavidin-conjugated horse radish peroxidase and 3,3′-diaminobenzidine substrate (Vectastain-ABC kit; Vector Laboratory, Burlingame, CA). (32). High resolution whole slide scanning was performed

using an Aperio ScanScope digital slide scanner (Carlsbad, CA) with the 40X objective as described (7). Sections in each experimental group were evaluated in a blinded fashion and representative fields identified.

**Cytokine and chemokine ELISA**

Virus infected brain supernatants were assessed for IL1β and IL6 levels using mouse IL1β ELISA ready-SET-Go (eBioscience # 88-7013) and IL6 ELISA ready-SET-Go (eBioscience # 88-7064), while CCL5 and CXCL10 levels were measured using mouse CCL5 ELISA kit (R&D systems # MMR00, Minneapolis, MN) and CXCL10 ELISA kit (R&D systems # MMR, Minneapolis, MN) according to the respective manufacturer's instructions. IFNγ in brain supernatants was measured by ELISA as described (22, 38). Briefly, 96-well plates were coated overnight at 4°C with 1 μg/ml rat anti-mouse IFNγ mAb (R4-6A2; BD Bioscience) in 100 μl 0.1M disodium hydrogen phosphate, pH 9.5, followed by blocking of nonspecific binding with 10% FCS in PBS for 1 h. Samples and recombinant IFNγ standard (BD Biosciences) were added overnight at 4°C. Bound IFNγ was detected using biotinylated rat anti-mouse IFNγ mAb (XMG1.2; BD Biosciences) and avidin peroxidase followed by 3,3′,5,5′ tetramethylbenzidine (TMB reagent set; BD Biosciences) 30 min later. Optical densities were read at 450 nm with a Bio-Rad model 680 microplate reader and analyzed using Microplate Manager 5.2 software (Bio-Rad Laboratories, Hercules, CA).

**Statistical analysis**

Survival curves and Real time PCR data were analyzed by unpaired, two-tailed Student t test. *, $P<0.05$. Data were analyzed using Microsoft Excel Software.

## Results

### Myd88 deficiency results in lethal viral encephalomyelitis.

To assess how Myd88 signaling affects pathogenesis associated with a demyelinating neurotropic virus, wt and Myd88$^{-/-}$ mice were infected with the sublethal, glia tropic coronavirus JHMV. Both groups of mice began to exhibit clinical signs of encephalitis at day 7 p.i., which progressed to partial or complete hind limb paralysis by day 10 p.i. (Fig. 1). Disease symptoms remained relatively stable in wt mice with recovery starting at day 14 p.i. By contrast, Myd88$^{-/-}$ suffered from more severe paralytic disease, which did not regress. In contrast to 90% survival of infected wt mice, Myd88$^{-/-}$ mice gradually succumbed to infection with a survival rate of only ~10% by day 21 (Fig. 1). Although Myd88 signaling did not alter the initial acute phase of viral encephalomyelitis, it affected clinical disease at the time coinciding with T cell mediated control of virus replication during days 7-14 p.i. in wt mice (22, 38, 44).

Analysis of viral load within the CNS demonstrated that the sustained disease severity of Myd88$^{-/-}$ mice correlated with ineffective virus control (Fig. 2). Whereas wt mice progressively reduced viral load between days 5 and 10 p.i., Myd88$^{-/-}$ mice already harbored higher viral loads at day 5 p.i. and showed no evidence of viral control until day 10 p.i., when virus titers exceeded those in wt mice by 3 $\log_{10}$ (Fig. 2A). Infectious virus was further modestly reduced in Myd88$^{-/-}$ mice surviving to day 14 p.i., at which time virus was already below detection in wt mice. Viral N mRNA levels in brains confirmed increased early virus replication and modest control by days 10 and 14 p.i. in Myd88$^{-/-}$ compared to wt mice (Fig. 2A). Similarly, viral mRNA levels in spinal cords were vastly increased by day 7 in infected Myd88$^{-/-}$ relative to wt mice, despite being similar at day 5 p.i. Differences remained prominent at days 10 and 14 p.i., when levels already

268 progressively declined in spinal cords of wt mice. Poorly controlled viral replication in spinal
269 cords was confirmed by ~2 $\log_{10}$ higher viral load in Myd88$^{-/-}$ relative to wt mice throughout days
270 10 to 14 p.i. (data not shown).

271 The glia tropic JHMV variant used herein is highly neurotropic with barely detectable
272 mRNA in the periphery of wt mice; however, it can disseminate to the liver in immune
273 compromised mice (20). Viral mRNA was measured in liver to determine if Myd88 deficiency
274 affected the immune system sufficiently to allow virus dissemination to the periphery. Viral
275 mRNA levels in the liver were similarly low at day 3 p.i. in both groups (Fig. 2B). However,
276 while viral mRNA levels remained sparse in liver at days 5 and 7 p.i. in wt mice compared to the
277 CNS, they increased by ~10 fold in the absence of Myd88 by day 5 p.i. Nevertheless, a
278 significant drop in viral mRNA by day 10 p.i. suggested control by adaptive immunity distinct
279 from the limited control of virus in the CNS. Furthermore, the absence of hepatitis, assessed by
280 lesion formation (data not shown), indicated liver infection did not contribute to mortality.

281 JHMV predominantly infects glia with very sparse neuronal tropism and rapidly
282 transitions from brain to spinal cord where virus is predominantly found within white matter
283 tracts (17, 34, 38, 56). To determine if Myd88 deficiency alters viral tropism, brains and spinal
284 cords were analyzed for the distribution of infected cells at days 7 and 10 p.i. (Fig. 3). In
285 contrast to the focal nature of infection in the brain of wt mice at day 7 p.i., the number of viral
286 antigen positive cells was markedly increased in infected Myd88$^{-/-}$ mice and the foci were much
287 more widely distributed throughout the brain (Fig. 3A). The dominant cell type infected in wt
288 mice exhibited a morphology consistent with glia/macrophages, although rare infected neurons
289 were also identified (Fig. 3A). Despite the increase in the number of infected cells in brains of
290 Myd88$^{-/-}$ mice, the relative proportion of infected glia to neurons remained similar. Striking

differences in distribution of virus antigen positive cells were also apparent in spinal cords (Fig. 3B). Whereas sections from wt mice only harbored few if any infected cells in white matter by day 10 p.i., Myd88$^{-/-}$ mice exhibited prominently increased numbers of infected cells in white matter, as well as viral dissemination to gray matter.

**Early IFNα/β expression in the CNS is Myd88 dependent**

IFNα/β is essential in preventing early JHMV dissemination within the CNS prior to emergence of adaptive immune responses (19). Elevated virus in the brain of Myd88$^{-/-}$ mice as early as day 5 p.i. thus implied impaired induction of IFNα/β and/or IFNα/β mediated antiviral factors. *Ifnα/β* mRNA expression in brains was analyzed as early as day 3 p.i., when virus replication was similar in both groups (Fig. 2). In wt mice *Ifnβ*, *Ifnα4* as well as *Ifnα5* transcripts all peaked at day 3 p.i., declined by day 5 p.i. and subsequently subsided to background levels (Fig. 4A), confirming previous results (19, 22). Although all three mRNA species were also increased over naïve levels in Myd88$^{-/-}$ mice, levels were significantly reduced relative to wt mice at day 3 p.i. All transcripts, particularly *Ifnβ* mRNA, subsequently increased by day 5 p.i. exceeding wt levels, and remained elevated in the absence of Myd88 to day 10 p.i. Consistent with the distinct *Ifnα/β* mRNA expression pattern, analysis of the IFN stimulated genes (ISG) *Ifit1*, *Ifit2* and *Isg15* also revealed impaired early induction in the brain, but subsequently higher transcript levels in the absence of Myd88 (Fig. 4B). The distinct kinetics and magnitude of *Ifnβ* mRNA in Myd88$^{-/-}$ relative to wt mice suggested Myd88 signaling contributes to very early IFNα/β induction, but that a Myd88-independent pathway is triggered as virus continues to replicate. Overall these results suggest that a Myd88 dependent IFNα/β activity stems early viral

spread within the CNS. However, subsequently impaired viral control in the absence of Myd88 is likely to reside in a defect in the adaptive immune response.

**Reduced proinflammatory factors in Myd88$^{-/-}$ mice correlate with impaired accumulation of neutrophils, macrophages and CD4 T cells**

Infections and sterile injury in Myd88$^{-/-}$ mice are both associated with reduced induction of pro-inflammatory cytokines and chemokines (2, 48, 53), even when IFNα/β induction is mainly driven by RIG-I and MDA5 (50). To assess if Myd88 deficiency affected proinflammatory factors during JHMV infection, brains were analyzed for cytokine and chemokine mRNA and protein expression throughout the acute phase of encephalomyelitis. IL1β, IL6 and TNF, commonly upregulated during acute neuroinflammation, promote disruption of the blood brain barrier (BBB) and facilitate CNS entry of leukocytes. In wt mice, *Il1β* and *Il6* mRNA levels were both maximal at day 3 p.i. (Fig.5A). Subsequently *Il1β* mRNA was sustained at high levels throughout day 7 p.i., while *Il6* mRNA progressively declined. Similar to *Ifnα/β* mRNA, induction of *Il1β* and *Il6* mRNA was impaired early in the absence of Myd88, but both mRNA levels increased by day 5 p.i., suggesting the early deficit was overcome by Myd88 independent signaling. Furthermore while *Il1β* mRNA continued to increase, *Il6* mRNA levels dropped by day 7 p.i., despite uncontrolled viral replication. *Tnf* mRNA was also significantly reduced at day 3 p.i. in the absence of Myd88, but was upregulated by day 5 p.i. and remained stable throughout day 10 p.i. CNS supernatants revealed reduced levels of IL1β in Myd88$^{-/-}$ mice as early as day 3 p.i. and even more distinctly at day 7 p.i., when expression peaked in wt mice (Fig. 5B). Similarly, IL6 was reduced by >50% in the absence of Myd88 at days 3 and 5 p.i. Moreover, while IL6 protein reflected mRNA levels in wt mice, it appeared post-

transcriptionally regulated in Myd88$^{-/-}$ mice. The discrepancy between mRNA and protein levels may reside in distinct translational regulation, e.g. impaired translation due to elevated levels of activated PKR coincident with elevated viral replication (22).

Chemokine transcripts associated with neutrophil, monocyte, and lymphocyte recruitment into the CNS were also examined (18). Transcripts encoding CXCL1, a neutrophil chemoattractant, as well as CCL2 and CCL3, both associated with monocyte recruitment, were all significantly impaired at day 3 p.i. in the absence of Myd88. However, while these transcripts declined by days 5 and 7 p.i. in wt mice, their delayed induction reached similar or even elevated levels in Myd88$^{-/-}$ brains (Fig. 6A). In wt mice transcripts encoding CCL5, CXCL10, and CXCL13, chemoattractants for T and B cells, were all induced by day 3 p.i., and *Ccl5* and *Cxcl13* mRNA continued to increase to day 7 p.i. By contrast, *Ccl5, Cxcl10,* and *Cxcl13* mRNA were barely detectable in Myd88$^{-/-}$ mice at day 3 p.i. While *Cxcl13* mRNA remained near baseline levels throughout day 10 p.i., *Ccl5* and *Cxcl10* mRNA induction were delayed in the absence of Myd88, but reached similar levels as in wt mice at days 10 and 7 p.i., respectively. Although *Cxcl10* mRNA dropped in both groups after day 7 p.i., levels remained higher in the absence of Myd88 at days 10 and 14 p.i., consistent with elevated virus and IFNα/β levels. CCL5 and CXCL10 in CNS homogenates reflected the patterns of mRNA (Fig. 6B). Both were significantly reduced in the absence of Myd88 at days 5 and 7 p.i. By day 10 p.i. CCL5 was equal and CXCL10 even higher compared to wt mice. The equilibration or even increased mRNA levels of chemokines after day 7 p.i., despite an early deficit in the absence of Myd88, presumably reflect sustained CNS virus load.

Consistent with impaired expression of proinflammatory chemokines, Myd88 deficiency is associated with reduced leukocyte recruitment into the CNS in various neuroinflammation

359 models (2, 25, 50, 53). During JHMV infection neutrophils and monocytes are early innate
360 responders that aid in subsequent parenchymal entry of T cells, although they do not directly
361 impact viral control or demyelination (44, 45). CD8 T cells are essential antiviral effectors via
362 IFNγ and perforin mediated mechanisms (27, 34). CD4 T cells contribute to antiviral
363 IFNγ production, promote local CD8 T cell effector function (37, 41), and are the major
364 producers of anti-inflammatory IL10 (42). We therefore assessed how the early impairment in
365 chemokine expression affected CNS leukocyte recruitment during JHMV infection. Infiltrating
366 $CD45^{hi}$ leukocytes were reduced by ~50% in $Myd88^{-/-}$ relative to wt mice at days 3 and 5 p.i., but
367 differences were less prominent by day 7 p.i. and thereafter (Fig. 7A). The deficit in early
368 inflammatory cells in $Myd88^{-/-}$ brains reflected a reduction in neutrophils ($CD45^{hi}$ $Ly6G^{+}$) by
369 >60%, and monocyte/macrophages ($CD45^{hi}$ $F480^{+}$) by >70% at days 3 and 5 p.i. (Fig. 7A),
370 supporting myeloid cells as early CNS infiltrates (44). Nevertheless, monocytes subsequently
371 increased (Fig. 7A), consistent with delayed expression of the chemoattractants CCL2 and CCL3
372 (Fig. 6A). Total numbers of CD4 and CD8 T cells in brains peaked between days 7 and 10 p.i. in
373 both groups (Fig. 7A). However, CD4 T cell recruitment was significantly impaired in the
374 absence of Myd88, reaching only 50% or less of wt levels throughout infection. By contrast,
375 Myd88 deficiency did not alter overall numbers of CD8 T cells or $tetramer^{+}$ CD8 T cells in the
376 CNS between days 7-14 p.i. (Fig. 7A). Myd88 signaling thus promoted early CNS accumulation
377 of myeloid cells and CD4 T cells, but did not affect CD8 T cell recruitment. Analysis of overall
378 inflammation by immunohistochemistry confirmed diminished recruitment of inflammatory
379 cells. Whereas wt mice showed numerous perivascular cuffs in the brain at day 7 p.i., areas of
380 perivascular inflammation were sparse and less pronounced in $Myd88^{-/-}$ mice (Fig. 7B).
381

**Myd88 deficiency impairs IFNγ production in the CNS**

Impaired CD4, yet similar CD8 T cell CNS infiltration in Myd88$^{-/-}$ mice suggested uncontrolled viral replication is due to inefficient T cell effector function (41). IFNγ, the most critical T cell derived antiviral mediator during JHMV infection (3, 17, 34), is more abundantly expressed by CD4 compared to CD8 T cells *in vivo* (39). In addition to its antiviral effect, IFNγ increases MHC expression on CNS target cells (4, 29), thus promoting both CD8 and CD4 T cell effector functions *in vivo*. In wt mice *Ifnγ* mRNA starts to accumulate at day 5 and peaks at day 7 p.i. (Fig. 8A), coincident with T cell accumulation and antiviral effector function within the CNS. Despite similar kinetics of *Ifnγ* mRNA expression in infected Myd88$^{-/-}$ and wt mice, levels were significantly reduced throughout acute infection in Myd88$^{-/-}$ mice. The pattern of IFNγ protein in the CNS matched that of mRNA in both groups (Fig. 8A). However, IFNγ was significantly lower in the CNS of Myd88$^{-/-}$ mice, specifically at day 7 p.i., when virus control by T cells is initially evident in wt mice. IFNγ production remained low by 10 p.i., despite the vastly increased viral load and similar levels of virus specific CD8 T cells in Myd88$^{-/-}$ mice (Fig. 7). Reduced IFNγ activity was supported by very sparse induction of IFNγ dependent *Nos2* mRNA in the CNS (Fig. 8). Low IFNγ levels also predicted impaired MHC upregulation, and consequently inefficient T cell engagement and effector activity. Class II expression was undetectable on microglia in uninfected controls (data not shown) as well as infected IFNγ deficient mice (4). Indeed, analysis of IFNγ dependent MHC class II expression on resident CD45$^{lo}$ microglia confirmed impaired class II upregulation in Myd88$^{-/-}$ mice (Fig. 8B). Consistent with the IFNγ kinetics, class II expression was low on microglia at day 5 p.i., but was increased on ~75% of microglia by day 7 p.i. Expression was sustained at day 10 p.i. in wt mice (Fig. 8B), despite the decline in IFNγ. By contrast, in Myd88$^{-/-}$ mice only 22% and 38% of

405 microglia expressed class II by day 7 p.i. and 10 p.i., respectively (Fig. 8B), reflecting reduced
406 IFNγ. Infiltrating macrophages ($CD45^{hi}$ $F480^{+}$) exhibited similarly impaired and delayed class II
407 expression in $Myd88^{-/-}$ mice compared to wt mice (data not shown). Decreased IFNγ in the CNS
408 of $Myd88^{-/-}$ mice was thus functionally evident by reduced *Nos2* mRNA and class II expression,
409 consistent with diminished accumulation and effector function of CD4 T cells (41).
410
411 **Myd88 signaling specifically promotes CD4 T cell function within the CNS**
412 The extent to which reduced IFNγ in the JHMV infected CNS was associated with CD4
413 or CD8 T cells was evaluated by *ex vivo* stimulation with the immunodominant $I\text{-}A^{b}$ restricted
414 M133 or $D^{b}$ restricted S510 peptide, respectively. Whereas ~25 % of CNS derived CD4 T cells
415 from wt mice produced IFNγ at days 7 and 10 p.i., only ~7% of the already lower $Myd88^{-/-}$ CD4
416 T cell population was capable of IFNγ production, representing a ~65-70% reduction in
417 frequency despite sustained high viral load (Fig. 9A). Importantly, stimulation of CNS derived
418 cells was carried out in the presence of class II expressing feeder cells, suggesting CD4 T cell
419 function was intrinsically impaired and not attributed to reduced class II expression *in vivo*.
420 Contrasting virus specific CD4 T cells, ~35% of CNS derived CD8 T cells produced IFNγ in
421 both groups of mice at day 7 (Fig. 9A) and 10 p.i. (data not shown), revealing no defects in
422 $Myd88^{-/-}$ CD8 T cells to produce IFNγ. This represented ~76% of $D^{b}$/S510 $tetramer^{+}$ CD8 T cells
423 and reflected similar percentages of tetramer reactive cells within the CD8 populations.
424 To assess whether defects in CD4 T cells were limited to the CNS, or imprinted during
425 activation in the periphery, T cells from the CLN, the anatomical site of T cell site priming
426 following JHMV infection (32), were examined at days 5 and 7 p.i. Overall frequencies of M133
427 specific CD4 T cells were below 2% in CLN of both groups; however, the percentage of IFNγ

428 producing cells was reduced by ~50% in Myd88$^{-/-}$ relative to wt populations (Fig. 9B). By
429 contrast, CLN CD8 T cells showed no differences in percentages of IFNγ producing cells at
430 either day 5 or 7 p.i. (Fig. 9B). Unimpaired virus specific CD8 T cell expansion in CLN was
431 confirmed by similar percentages of S510 tetramer$^{+}$ CD8 T cells (~1% in both wt and Myd88$^{-/-}$
432 CD8 T cells at day 7 p.i. (data not shown). These results imply that reduced IFNγ in the CNS of
433 JHMV infected Myd88$^{-/-}$ mice is not only associated with reduced recruitment/survival of CD4 T
434 cells, but also severely impaired IFNγ production by CD4 T cells. Moreover, the defect in CD4 T
435 cell responsiveness is already imprinted during the priming/expansion phase in the CLN, and is
436 exacerbated further in the CNS.
437
438 **Uncontrolled virus replication in the absence of Myd88 coincides with increased**
439 **demyelination despite limited inflammation.**
440 A hallmark of JHMV infection in wt mice is T cell driven immune mediated
441 demyelination (3, 56, 58). In contrast to immune competent mice, mice deficient in T and B cells
442 do not develop demyelinating disease, despite the inability to control infectious virus (58). To
443 assess how reduced T cell effector function in Myd88$^{-/-}$ mice influences JHMV mediated
444 pathology, demyelination was assessed in brain and spinal cord. Interestingly, JHMV infected
445 Myd88$^{-/-}$ mice exhibited pronounced demyelination in the brain stem by day 10 p.i. (Fig. 10). By
446 contrast, demyelination was very limited in brains of wt mice. Although demyelination was
447 clearly evident in the spinal cords of wt mice at day 14 p.i., the extent of demyelination in the
448 spinal cord was prominently increased in the absence of Myd88 signaling (Fig. 10).
449

**Discussion**

Myd88 signaling is involved in induction of type I IFN, proinflammatory factors and leukocyte recruitment to the CNS in various neuroinflammation models including microbial infection as well as stab wound injury (2, 8, 16, 50, 53). However, the effects exerted by Myd88 depend on the insult, and can be disassociated from IFNα/β induction if viruses are predominantly sensed by Myd88-independent PRRs (50). Coronaviruses, including MHV, are very poor inducers of IFNα/β in most cell types, which has been attributed to the similarity of the capped viral mRNA to host mRNA (62). Nevertheless IFNα/β is critical to block viral dissemination in both the CNS and periphery (9, 19). Results in this study demonstrate that Myd88 is essential for control of CNS infection by the sublethal gliatropic coronavirus JHMV. Moreover, protection from lethal encephalomyelitis via Myd88 signaling was mediated at both the innate and adaptive immune levels.

Early during JHMV infection Myd88 deficiency significantly impaired initial induction of IFNα/β and downstream transcription of ISGs. As virus continued to replicate impaired IFNα/β induction was overcome by Myd88-independent signals. Nevertheless, the failure to rapidly establish a protective antiviral state provided a window for viral dissemination within the CNS prior to recruitment of adaptive immune cells. Myd88- independent IFNα/β production, although delayed, is consistent with the notion that MHV infection of glia is mainly sensed by cytosolic PRRs. MDA5 is the main sensor required to induce IFNα/β in microglia/macrophages following infection with the MHV-A59 strain (43), while both MDA5 and RIG-I sense MHV-A59 in an oligodendroglial cell line (26). However, although oligodendrocytes are major targets of JHMV, they do not induce IFNα/β in response to JHMV *in vivo* (21). Delayed yet increased IFNα/β induction in the Myd88$^{-/-}$ CNS is thus likely attributed to MDA5 activation in infected

microglia/macrophages. The failure to limit viral spread despite enhanced Myd88 independent IFNα/β responses presumably resides in the viruses ability to outpace IFNα/β mediated protection, similar to uncontrolled infection in SCID or Rag deficient mice (5, 36).

The contributions of Myd88 to promoting innate and adaptive immunity during CNS infections associated with the cytosolic sensors RIG-I and MDA5 are only sparsely explored. Despite the overall paucity of IFNα/β induction by evasion of MDA5 recognition, plasmacytoid dendritic cells (pDCs) make a critical contribution to TLR7 mediated IFNα/β induction following peripheral infection with MHV-A59 (9). While we cannot exclude a contribution of pDC in the CNS to early IFNα/β production, minimal peripheral replication of the gliatropic JHMV, relative to MHV-A59, is less likely to activate pronounced pDC signaling. Moreover, although recruitment of pDCs to the CNS has been demonstrated (6, 24, 59), it has not been described during MHV infection. We thus favor the notion that non viral factors such as cellular stress responses may contribute to triggering Myd88 dependent innate responses (47). Moreover, other resident cells infected early such as ependymal cells (55), may contribute to the early innate response.

Myd88 was also essential for early induction of numerous proinflammatory factors, including IL1β, IL6, TNF and various chemokines. Similar to delayed IFNα/β responses, the diminished proinflammatory responses were, for the most part, overcome by day 7 p.i. and correlated with uncontrolled virus replication. It remains to be elucidated whether IFNα/β and innate proinflammatory factors are activated via similar temporally distinct Myd88 and Myd88 independent pathways. However in this context it is interesting to note that Myd88 deficiency was only associated with a defect in chemokines, but not IFNα/β production in the CNS following WNV infection (50). Neither expression of systemic IFNα/β nor *Ifnα/β* mRNA were

496 impaired in cerebral cortex of WNV infected Myd88$^{-/-}$ relative to wt mice at day 6 p.i. However,
497 WNV load was elevated in the absence of Myd88 in several anatomical CNS regions as early as
498 day 4 p.i. As corresponding *Ifnα/β* mRNA levels were not provided at this early time, it remains
499 unclear whether enhanced WNV replication was solely due to the absence of a Myd88 mediated
500 antiviral activity independent of IFNα/β (50).

501 Consistent with delayed and blunted induction of proinflammatory mediators and the
502 chemokines CXCL1, CCL2, and CCL5, recruitment of neutrophils and monocytes into the CNS
503 was significantly dampened in JHMV infected Myd88$^{-/-}$ mice during the innate response.
504 Neutrophils and monocytes play subtle roles during JHMV infection by accelerating leukocyte
505 entry into the CNS parenchyma. Although abrogation of either myeloid subset alone does not
506 significantly impair viral control or pathology (44), we cannot exclude that reduced recruitment
507 of these myeloid populations may contribute to enhanced pathogenesis in Myd88$^{-/-}$ mice.
508 Furthermore, impaired CXCL10, coincident with a defect in CD4 T cell accumulation, is
509 consistent with a prominent role of CXCL10 in promoting CD4, but not CD8 T cell recruitment
510 into the CNS (28, 31). Importantly, impaired IFNγ production by virus specific CD4 T cells
511 directly correlated with uncontrolled viral replication after day 5 p.i. Early CD4 T cell mediated
512 IFNγ production enhances both class I and class II MHC upregulation (4, 29, 38). Although
513 neither total nor virus specific CD8 T cell accumulation were affected by Myd88 deficiency,
514 reduced antigen presentation by CNS resident cells and CD4 T cell help may limit CD8 T cell
515 function *in vivo*. Indeed, CD4 T cells are critical to promote CD8 function within the CNS
516 during JHMV infection (41), partially by prolonging CD8 T cell activity via IL21 production
517 (37). *Il21* mRNA, expressed mainly by CD4 T cells, was reduced by ~40% in the CNS at day 7
518 p.i. in the absence of Myd88. Although CD8 T cell function was not affected *ex vivo*, a

519 contribution of impaired CD4 T cell help to limited CD8 T cell function *in vivo* cannot be
520 excluded. Finally, NK cells are redundant for JHMV pathogenesis (61), supporting insufficient
521 CD4 T cell activation as a critical Myd88 dependent component in viral control within the CNS.
522 Myeloid and total T cell, but not virus specific CD8 T cell accumulation was also blunted
523 in the CNS of WNV infected Myd88$^{-/-}$ mice, although peripheral T cell responses were not
524 impaired (50). Similar to JHMV infection, virus control was primarily affected in the CNS and
525 not periphery. Myd88$^{-/-}$ mice are also highly susceptible to cerebral infection by *Toxoplasma*
526 *gondii* (53). Increased parasite burden and severe pathology in the CNS is also directly
527 correlated with reduced expression of proinflammatory molecules and local production of IFNγ,
528 a mediator of protective immunity. In this case impaired IFNγ coincided with significantly
529 decreased recruitment of CD8 T cells. However, contrasting JHMV infection, CNS accumulation
530 of myeloid cells was increased relative to wt mice (53), suggesting Myd88 signaling can also
531 inhibit CNS inflammation in some circumstances.
532 The mechanisms underlying impaired T cell function in the absence of Myd88 have
533 recently been explored during WNV induced encephalitis. Consistent with unimpaired peripheral
534 responses in Myd88$^{-/-}$ mice, IL1R deficiency did not impair peripheral T cell activation or T cell
535 recruitment into the CNS (11). IL1R signaling was rather specifically required to reactivate T
536 cells by promoting maturation of antigen presenting cells (APC) within the CNS. Defective T
537 cell antiviral activity within the CNS was thus attributed to impaired local reactivation in contrast
538 to a defect at the priming stage in the periphery (12). A similar mechanism involving IL1R
539 dependent infiltrating APC may underlie poor CD4 T cell responses following JHMV infection.
540 However, defective CD4 T cell responses were already evident in CLN during priming,
541 consistent with the ability of IL1β to induce both phagocytosis and antigen-presenting function



Journal of Virology

542 during monocyte differentiation (46). The APC reactivating JHMV specific CD4 T cells in the
543 CNS have not been identified; however, JHMV only poorly infects dendritic cells (60).
544 Moreover, while microglia and macrophages are both infected, they require IFNγ for class II
545 upregulation. As oligodendrocytes, the most prominent cell type infected in wt mice do not
546 express class II, CD4 T cells are most likely activated by cross presentation (1).

547 An unanticipated result was the increased extent of demyelination in both the brain and
548 spinal cord of JHMV infected Myd88$^{-/-}$ mice, despite more limited induction of proinflammatory
549 factors and reduced inflammatory infiltrates. Although it can be argued that enhanced
550 demyelination results from uncontrolled viral load and direct virus induced oligodendrocyte
551 damage, demyelination is very sparse in mice devoid of adaptive immune responses (14, 55).
552 Moreover, enhanced oligodendrocyte infection in mice incapable of responding to IFNγ
553 specifically in oligodendrocytes does not lead to increased demyelination despite effective T cell
554 function (17). This suggests a protective function of Myd88 in demyelination independent of
555 viral load in oligodendrocytes. While Myd88 is also redundant for spontaneous autoimmune
556 mediated demyelination (57), it is essential to mediate experimental allergic encephalomyelitis
557 following autoantigen immunization (33). These diverse results implicate distinct contributions
558 of Myd88 to demyelination depending on the local environment and responder cell types.

559 In summary the present study reveals that Myd88 protects from lethal JHMV
560 encephalomyelitis by at least two pathways. During the innate phase, Myd88 promotes initial
561 induction of IFNα/β, thereby stemming viral dissemination within the CNS and spread to the
562 liver prior to expansion of virus specific T cells. Although the impaired early innate responses
563 overcome, Myd88 is essential in promoting activation of virus specific CD4 T cells in CLN, as
564 well as enhancing their accumulation and IFNγ secretion within the CNS. Analogous to WNV

565 and *toxoplasma gondii* induced encephalitis, these data support a vital role of Myd88 signaling in
566 protective antimicrobial function in the CNS by promoting early induction of proinflammatory
567 mediators as well as supporting T cell mediated IFNγ production.
568
569 **Acknowledgements**
570 This study was supported by National Institute of Health Grant P01 NS064932. We sincerely
571 thank Wenqiang Wei, Eric Barron, and Ernesto Barron for exceptional technical assistance with
572 histopathology.
573
574 **Footnote**
575 This paper is dedicated to Niranjan Butchi and his family.
576

## Figure Legends

**Figure 1. Myd88$^{-/-}$ mice exhibit severe clinical disease and succumb to JHMV infection.** wt and Myd88$^{-/-}$ mice infected intracranially with JHMV were monitored for clinical disease as described in methods (top panel) and survival (bottom panel). Clinical scores represent the average of two independent experiments ($n \geq 20$) ± SEM. *, $P < 0.05$. Survival rates (n =18 per group) are representative of two independent experiments.

**Figure 2. Myd88 deficiency impairs CNS viral control.** Virus replication in brain, spinal cord and liver of infected wt and Myd88$^{-/-}$ mice was determined by plaque assay or quantitative real-time PCR analysis of viral N protein encoding transcripts as indicated. Levels of viral mRNA were determined relative to *Gapdh*. Data represent the average of two-three independent experiments (n=6-9) ± SEM. *, $P<0.05$.

**Figure 3. Myd88 deficiency enhances virus dissemination within the CNS.** Viral antigen detected using mAb specific for viral N protein in brain (A) and spinal cord (B) of infected wt and Myd88$^{-/-}$ mice at days 7 and 14 p.i., respectively. Note increased foci of viral antigen-positive cells in Myd88$^{-/-}$ mice. Insets show infected cells at higher magnification. Bars in (A), 1 mm, 100 μm (inserts). Bars in (B), 500 μm, 50 μm (inserts).

**Figure 4. Delayed type I interferon and IFN stimulated gene expression in the CNS of Myd88$^{-/-}$ mice.** Expression of *Ifnβ*, *Ifna4 and Ifna5* mRNA (A) and IFNα/β inducible genes *Ifit1, Ifit2* and *Isg15* (B) relative to *Gapdh* in brains of naïve and JHMV infected wt and Myd88$^{-/-}$ mice determined by real time PCR. Data represented the average ± SEM (n=6 mice/group/time-point) from two separate experiments. Naïve values are shown for wt mice and represent n=3. *$P<0.05$.

**Figure 5. Reduced pro-inflammatory cytokine response in absence of Myd88.** (A) *Il1β, Il6* and *Tnf* mRNA levels relative to *Gapdh* in brains of naïve and JHMV infected wt and Myd88$^{-/-}$ mice determined by real time PCR. Data represent the average ± SEM of n=6 mice/group/time-point from two separate experiments. Naïve values are shown for wt mice and represent n=3. (B) IL1β and IL6 protein in brain supernatants of infected wt and Myd88$^{-/-}$ mice determined by ELISA. Data are average ± SEM of two independent experiments. (n = 6/group). *$P<0.05$.

**Figure 6. Impaired chemokine expression in absence of Myd88.** (A) Expression of *Cxcl1*, *Ccl2* and *Ccl3, Ccl5, Cxcl10* and *Cxcl13* mRNA relative to *Gapdh* in brains of infected wt and Myd88$^{-/-}$ mice determined by real time PCR. Data from naïve wt mice represents n=3. (B) Protein level of T cell chemo-attractants CCL5 and CXCL10 in brain supernatants from infected wt and Myd88$^{-/-}$ mice determined by ELISA. Data represent average ± SEM of two independent experiments (n= 6/group). *$P<0.05$.

**Figure 7. Myd88 deficiency impairs CNS recruitment of myeloid and CD4 T cells. (A)** Numbers of total infiltrating leukocytes (CD45$^{hi}$), neutrophils (Ly6G$^{+}$), macrophages (F480$^{+}$), CD4 T cells, CD8 T cells and virus specific D$^{b}$/S510 tetramer reactive CD8 T cells in the CNS of infected wt and Myd88$^{-/-}$ mice determined by flow cytometry at indicated times p.i.. Data represent the mean ± SEM of pooled mice (n=6/group/time-point and experiment) from three

separate experiments. *P<0.05. (B) Representative inflammation determined by hematoxylin and eosin staining in brain at day 7 p.i. Data are representative of 3 – 4 individuals from 2 separate experiments. Insets show perivascular areas at higher magnification. Bars, 500 μm, 50 μm (inserts).

**Figure 8. Defective IFNγ and MHC class II upregulation in the CNS of Myd88$^{-/-}$ mice.** (A) Expression of *Ifnγ* mRNA, IFNγ protein, and IFNγ inducible *Nos2* mRNA in brains of naïve and infected wt and Myd88$^{-/-}$ mice at the indicated times. Transcript levels were measured by real time PCR relative to *Gapdh* and protein levels by ELISA. Data represents the mean ± SEM from two independent experiments (n=6). Data from naïve wt mice represents n=3. *, P<0.05. (B) Upregulation of MHC class II on brain microglia following JHMV infection in wt and Myd88-/- mice determined by flow cytometry. CNS derived cells pooled from infected wt and Myd88-/- mice at days 5, 7 and 10 p.i. (n=4-5) were stained with anti-CD45 and anti-class II I-A/E. Density plots are gated on total CD45$^{+}$ cells; quadrants are set to separate class II positive microglia (CD45$^{low}$) from infiltrating (CD45$^{high}$) cells as indicated. Numbers in parenthesis represent percentages of class II expressing cells within microglia. Data is representative of three independent experiments ± SEM.

**Figure 9. Myd88 signaling is critical for regulating virus specific CD4 but not CD8 T cell activity**. Cells from brains (A) or CLN (B) of infected wt and Myd88$^{-/-}$ mice harvested at the indicated times were analyzed for frequencies of IFNγ producing CD8 or CD4 T cells in response to S510 or M133 peptide stimulation, respectively. Representative density plots of brain derived cells are gated on CD4 or CD8 T cells in the absence (-) or presence (+) of peptide. IFNγ producing cells are depicted in rectangles and numbers show relative percentages of IFNγ$^{+}$ cells. Bar graphs show average frequencies ± SEM of IFNγ producing cells within CD4 or CD8 T cells from 3 individual mice. *P<0.05.

**Fig. 10. Myd88 deficiency enhances demyelination.** Brain stems at day 10 (top panel) and spinal cords at day 14 p.i. (lower panel) of infected wt and Myd88$^{-/-}$ mice stained with LFB . Data are representative of 2 separate experiments with 3 – 4 individuals per experiment and 6 cross sections per cord. Bars, 500 μm.

## References


1. **Aleyas, A. G., Y. W. Han, A. M. Patil, S. B. Kim, K. Kim, and S. K. Eo.** 2012. Impaired cross-presentation of CD8alpha+ CD11c+ dendritic cells by Japanese encephalitis virus in a TLR2/MyD88 signal pathway-dependent manner. Eur J Immunol **42:**2655-2666.
2. **Babcock, A. A., H. Toft-Hansen, and T. Owens.** 2008. Signaling through MyD88 regulates leukocyte recruitment after brain injury. J Immunol **181:**6481-6490.
3. **Bergmann, C. C., T. E. Lane, and S. A. Stohlman.** 2006. Coronavirus infection of the central nervous system: host-virus stand-off. Nat Rev Microbiol **4:**121-132.
4. **Bergmann, C. C., B. Parra, D. R. Hinton, R. Chandran, M. Morrison, and S. A. Stohlman.** 2003. Perforin-mediated effector function within the central nervous system requires IFN-gamma-mediated MHC up-regulation. J Immunol **170:**3204-3213.
5. **Bergmann, C. C., B. Parra, D. R. Hinton, C. Ramakrishna, K. C. Dowdell, and S. A. Stohlman.** 2004. Perforin and gamma interferon-mediated control of coronavirus central nervous system infection by CD8 T cells in the absence of CD4 T cells. J Virol **78:**1739-1750.
6. **Brehin, A. C., J. Mouries, M. P. Frenkiel, G. Dadaglio, P. Despres, M. Lafon, and T. Couderc.** 2008. Dynamics of immune cell recruitment during West Nile encephalitis and identification of a new CD19+B220-BST-2+ leukocyte population. J Immunol **180:**6760-6767.
7. **Butchi, N. B., D. R. Hinton, S. A. Stohlman, P. Kapil, V. Fensterl, G. C. Sen, and C. C. Bergmann.** 2014. Ifit2 deficiency results in uncontrolled neurotropic coronavirus replication and enhanced encephalitis via impaired alpha/beta interferon induction in macrophages. J Virol **88:**1051-1064.
8. **Carty, M., L. Reinert, S. R. Paludan, and A. G. Bowie.** 2014. Innate antiviral signalling in the central nervous system. Trends Immunol **35:**79-87.
9. **Cervantes-Barragan, L., R. Zust, F. Weber, M. Spiegel, K. S. Lang, S. Akira, V. Thiel, and B. Ludewig.** 2007. Control of coronavirus infection through plasmacytoid dendritic-cell-derived type I interferon. Blood **109:**1131-1137.
10. **Cho, H., S. C. Proll, K. J. Szretter, M. G. Katze, M. Gale, Jr., and M. S. Diamond.** 2013. Differential innate immune response programs in neuronal subtypes determine susceptibility to infection in the brain by positive-stranded RNA viruses. Nat Med **19:**458-464.
11. **Durrant, D. M., B. P. Daniels, and R. S. Klein.** 2014. IL-1R1 signaling regulates CXCL12-mediated T cell localization and fate within the central nervous system during West Nile Virus encephalitis. J Immunol **193:**4095-4106.
12. **Durrant, D. M., M. L. Robinette, and R. S. Klein.** 2013. IL-1R1 is required for dendritic cell-mediated T cell reactivation within the CNS during West Nile virus encephalitis. J Exp Med **210:**503-516.
13. **Fleming, J. O., M. D. Trousdale, F. A. el-Zaatari, S. A. Stohlman, and L. P. Weiner.** 1986. Pathogenicity of antigenic variants of murine coronavirus JHM selected with monoclonal antibodies. J Virol **58:**869-875.

14. **Fleming, J. O., F. I. Wang, M. D. Trousdale, D. R. Hinton, and S. A. Stohlman.** 1993. Interaction of immune and central nervous systems: contribution of anti-viral Thy-1+ cells to demyelination induced by coronavirus JHM. Reg Immunol **5:**37-43.
15. **Fredericksen, B. L., B. C. Keller, J. Fornek, M. G. Katze, and M. Gale, Jr.** 2008. Establishment and maintenance of the innate antiviral response to West Nile Virus involves both RIG-I and MDA5 signaling through IPS-1. J Virol **82:**609-616.
16. **Furr, S. R., and I. Marriott.** 2012. Viral CNS infections: role of glial pattern recognition receptors in neuroinflammation. Front Microbiol **3:**201.
17. **Gonzalez, J. M., C. C. Bergmann, C. Ramakrishna, D. R. Hinton, R. Atkinson, J. Hoskin, W. B. Macklin, and S. A. Stohlman.** 2006. Inhibition of interferon-gamma signaling in oligodendroglia delays coronavirus clearance without altering demyelination. Am J Pathol **168:**796-804.
18. **Hosking, M. P., and T. E. Lane.** 2010. The role of chemokines during viral infection of the CNS. PLoS Pathog **6:**e1000937.
19. **Ireland, D. D., S. A. Stohlman, D. R. Hinton, R. Atkinson, and C. C. Bergmann.** 2008. Type I interferons are essential in controlling neurotropic coronavirus infection irrespective of functional CD8 T cells. J Virol **82:**300-310.
20. **Ireland, D. D., S. A. Stohlman, D. R. Hinton, P. Kapil, R. H. Silverman, R. A. Atkinson, and C. C. Bergmann.** 2009. RNase L mediated protection from virus induced demyelination. PLoS Pathog **5:**e1000602.
21. **Kapil, P., N. B. Butchi, S. A. Stohlman, and C. C. Bergmann.** 2012. Oligodendroglia are limited in type I interferon induction and responsiveness in vivo. Glia **60:**1555-1566.
22. **Kapil, P., S. A. Stohlman, D. R. Hinton, and C. C. Bergmann.** 2014. PKR mediated regulation of inflammation and IL-10 during viral encephalomyelitis. J Neuroimmunol **270:**1-12.
23. **Kurt-Jones, E. A., M. Chan, S. Zhou, J. Wang, G. Reed, R. Bronson, M. M. Arnold, D. M. Knipe, and R. W. Finberg.** 2004. Herpes simplex virus 1 interaction with Toll-like receptor 2 contributes to lethal encephalitis. Proc Natl Acad Sci U S A **101:**1315-1320.
24. **Lande, R., V. Gafa, B. Serafini, E. Giacomini, A. Visconti, M. E. Remoli, M. Severa, M. Parmentier, G. Ristori, M. Salvetti, F. Aloisi, and E. M. Coccia.** 2008. Plasmacytoid dendritic cells in multiple sclerosis: intracerebral recruitment and impaired maturation in response to interferon-beta. J Neuropathol Exp Neurol **67:**388-401.
25. **Lang, K. S., A. A. Navarini, M. Recher, P. A. Lang, M. Heikenwalder, B. Stecher, A. Bergthaler, B. Odermatt, S. Akira, K. Honda, H. Hengartner, and R. M. Zinkernagel.** 2007. MyD88 protects from lethal encephalitis during infection with vesicular stomatitis virus. Eur J Immunol **37:**2434-2440.
26. **Li, J., Y. Liu, and X. Zhang.** 2010. Murine coronavirus induces type I interferon in oligodendrocytes through recognition by RIG-I and MDA5. J Virol **84:**6472-6482.
27. **Lin, M. T., S. A. Stohlman, and D. R. Hinton.** 1997. Mouse hepatitis virus is cleared from the central nervous systems of mice lacking perforin-mediated cytolysis. J Virol **71:**383-391.
28. **Liu, M. T., H. S. Keirstead, and T. E. Lane.** 2001. Neutralization of the chemokine CXCL10 reduces inflammatory cell invasion and demyelination and improves neurological function in a viral model of multiple sclerosis. J Immunol **167:**4091-4097.

29. **Malone, K. E., S. A. Stohlman, C. Ramakrishna, W. Macklin, and C. C. Bergmann.** 2008. Induction of class I antigen processing components in oligodendroglia and microglia during viral encephalomyelitis. Glia **56:**426-435.

30. **Mansur, D. S., E. G. Kroon, M. L. Nogueira, R. M. Arantes, S. C. Rodrigues, S. Akira, R. T. Gazzinelli, and M. A. Campos.** 2005. Lethal encephalitis in myeloid differentiation factor 88-deficient mice infected with herpes simplex virus 1. Am J Pathol **166:**1419-1426.

31. **Marques, C. P., P. Kapil, D. R. Hinton, C. Hindinger, S. L. Nutt, R. M. Ransohoff, T. W. Phares, S. A. Stohlman, and C. C. Bergmann.** 2011. CXCR3-dependent plasma blast migration to the central nervous system during viral encephalomyelitis. J Virol **85:**6136-6147.

32. **Marten, N. W., S. A. Stohlman, J. Zhou, and C. C. Bergmann.** 2003. Kinetics of virus-specific CD8+ -T-cell expansion and trafficking following central nervous system infection. J Virol **77:**2775-2778.

33. **Miranda-Hernandez, S., N. Gerlach, J. M. Fletcher, E. Biros, M. Mack, H. Korner, and A. G. Baxter.** 2011. Role for MyD88, TLR2 and TLR9 but not TLR1, TLR4 or TLR6 in experimental autoimmune encephalomyelitis. J Immunol **187:**791-804.

34. **Parra, B., D. R. Hinton, N. W. Marten, C. C. Bergmann, M. T. Lin, C. S. Yang, and S. A. Stohlman.** 1999. IFN-gamma is required for viral clearance from central nervous system oligodendroglia. J Immunol **162:**1641-1647.

35. **Paul, S., C. Ricour, C. Sommereyns, F. Sorgeloos, and T. Michiels.** 2007. Type I interferon response in the central nervous system. Biochimie **89:**770-778.

36. **Pewe, L., and S. Perlman.** 2002. Cutting edge: CD8 T cell-mediated demyelination is IFN-gamma dependent in mice infected with a neurotropic coronavirus. J Immunol **168:**1547-1551.

37. **Phares, T. W., K. D. DiSano, D. R. Hinton, M. Hwang, A. J. Zajac, S. A. Stohlman, and C. C. Bergmann.** 2013. IL-21 optimizes T cell and humoral responses in the central nervous system during viral encephalitis. J Neuroimmunol **263:**43-54.

38. **Phares, T. W., C. Ramakrishna, G. I. Parra, A. Epstein, L. Chen, R. Atkinson, S. A. Stohlman, and C. C. Bergmann.** 2009. Target-dependent B7-H1 regulation contributes to clearance of central nervous system infection and dampens morbidity. J Immunol **182:**5430-5438.

39. **Phares, T. W., S. A. Stohlman, D. R. Hinton, R. Atkinson, and C. C. Bergmann.** 2010. Enhanced antiviral T cell function in the absence of B7-H1 is insufficient to prevent persistence but exacerbates axonal bystander damage during viral encephalomyelitis. J Immunol **185:**5607-5618.

40. **Phares, T. W., S. A. Stohlman, D. R. Hinton, and C. C. Bergmann.** 2012. Enhanced CD8 T-cell anti-viral function and clinical disease in B7-H1-deficient mice requires CD4 T cells during encephalomyelitis. J Neuroinflammation **9:**269.

41. **Phares, T. W., S. A. Stohlman, M. Hwang, B. Min, D. R. Hinton, and C. C. Bergmann.** 2012. CD4 T cells promote CD8 T cell immunity at the priming and effector site during viral encephalitis. J Virol **86:**2416-2427.

42. **Puntambekar, S. S., C. C. Bergmann, C. Savarin, C. L. Karp, T. W. Phares, G. I. Parra, D. R. Hinton, and S. A. Stohlman.** 2011. Shifting hierarchies of interleukin-10-producing T cell populations in the central nervous system during acute and persistent viral encephalomyelitis. J Virol **85:**6702-6713.

43. **Roth-Cross, J. K., S. J. Bender, and S. R. Weiss.** 2008. Murine coronavirus mouse hepatitis virus is recognized by MDA5 and induces type I interferon in brain macrophages/microglia. J Virol **82:**9829-9838.
44. **Savarin, C., S. A. Stohlman, R. Atkinson, R. M. Ransohoff, and C. C. Bergmann.** 2010. Monocytes regulate T cell migration through the glia limitans during acute viral encephalitis. J Virol **84:**4878-4888.
45. **Savarin, C., S. A. Stohlman, A. M. Rietsch, N. Butchi, R. M. Ransohoff, and C. C. Bergmann.** 2011. MMP9 deficiency does not decrease blood-brain barrier disruption, but increases astrocyte MMP3 expression during viral encephalomyelitis. Glia **59:**1770-1781.
46. **Schenk, M., M. Fabri, S. R. Krutzik, D. J. Lee, D. M. Vu, P. A. Sieling, D. Montoya, P. T. Liu, and R. L. Modlin.** 2014. Interleukin-1beta triggers the differentiation of macrophages with enhanced capacity to present mycobacterial antigen to T cells. Immunology **141:**174-180.
47. **Smith, J. A.** 2014. A new paradigm: innate immune sensing of viruses via the unfolded protein response. Front Microbiol **5:**222.
48. **Sorensen, L. N., L. S. Reinert, L. Malmgaard, C. Bartholdy, A. R. Thomsen, and S. R. Paludan.** 2008. TLR2 and TLR9 synergistically control herpes simplex virus infection in the brain. J Immunol **181:**8604-8612.
49. **Suthar, M. S., D. Y. Ma, S. Thomas, J. M. Lund, N. Zhang, S. Daffis, A. Y. Rudensky, M. J. Bevan, E. A. Clark, M. K. Kaja, M. S. Diamond, and M. Gale, Jr.** 2010. IPS-1 is essential for the control of West Nile virus infection and immunity. PLoS Pathog **6:**e1000757.
50. **Szretter, K. J., S. Daffis, J. Patel, M. S. Suthar, R. S. Klein, M. Gale, Jr., and M. S. Diamond.** 2010. The innate immune adaptor molecule MyD88 restricts West Nile virus replication and spread in neurons of the central nervous system. J Virol **84:**12125-12138.
51. **Takeuchi, O., and S. Akira.** 2010. Pattern recognition receptors and inflammation. Cell **140:**805-820.
52. **Thompson, M. R., J. J. Kaminski, E. A. Kurt-Jones, and K. A. Fitzgerald.** 2011. Pattern recognition receptors and the innate immune response to viral infection. Viruses **3:**920-940.
53. **Torres, M., R. Guiton, S. Lacroix-Lamande, B. Ryffel, S. Leman, and I. Dimier-Poisson.** 2013. MyD88 is crucial for the development of a protective CNS immune response to Toxoplasma gondii infection. J Neuroinflammation **10:**19.
54. **Town, T., F. Bai, T. Wang, A. T. Kaplan, F. Qian, R. R. Montgomery, J. F. Anderson, R. A. Flavell, and E. Fikrig.** 2009. Toll-like receptor 7 mitigates lethal West Nile encephalitis via interleukin 23-dependent immune cell infiltration and homing. Immunity **30:**242-253.
55. **Wang, F. I., D. R. Hinton, W. Gilmore, M. D. Trousdale, and J. O. Fleming.** 1992. Sequential infection of glial cells by the murine hepatitis virus JHM strain (MHV-4) leads to a characteristic distribution of demyelination. Lab Invest **66:**744-754.
56. **Wang, F. I., S. A. Stohlman, and J. O. Fleming.** 1990. Demyelination induced by murine hepatitis virus JHM strain (MHV-4) is immunologically mediated. J Neuroimmunol **30:**31-41.
57. **Wexler, A. G., C. Frielle, G. Berry, L. R. Budgeon, J. Baccon, N. D. Christensen, and H. Waldner.** 2013. The innate immune adaptor MyD88 is dispensable for

spontaneous autoimmune demyelination in a mouse model of multiple sclerosis. J Neuroimmunol **255:**60-69.

58. **Wu, G. F., A. A. Dandekar, L. Pewe, and S. Perlman.** 2000. CD4 and CD8 T cells have redundant but not identical roles in virus-induced demyelination. J Immunol **165:**2278-2286.

59. **Wuest, T. R., and D. J. Carr.** 2008. Dysregulation of CXCR3 signaling due to CXCL10 deficiency impairs the antiviral response to herpes simplex virus 1 infection. J Immunol **181:**7985-7993.

60. **Zhou, H., and S. Perlman.** 2006. Preferential infection of mature dendritic cells by mouse hepatitis virus strain JHM. J Virol **80:**2506-2514.

61. **Zuo, J., S. A. Stohlman, J. B. Hoskin, D. R. Hinton, R. Atkinson, and C. C. Bergmann.** 2006. Mouse hepatitis virus pathogenesis in the central nervous system is independent of IL-15 and natural killer cells. Virology **350:**206-215.

62. **Zust, R., L. Cervantes-Barragan, M. Habjan, R. Maier, B. W. Neuman, J. Ziebuhr, K. J. Szretter, S. C. Baker, W. Barchet, M. S. Diamond, S. G. Siddell, B. Ludewig, and V. Thiel.** 2011. Ribose 2'-O-methylation provides a molecular signature for the distinction of self and non-self mRNA dependent on the RNA sensor Mda5. Nat Immunol **12:**137-143.

*1*

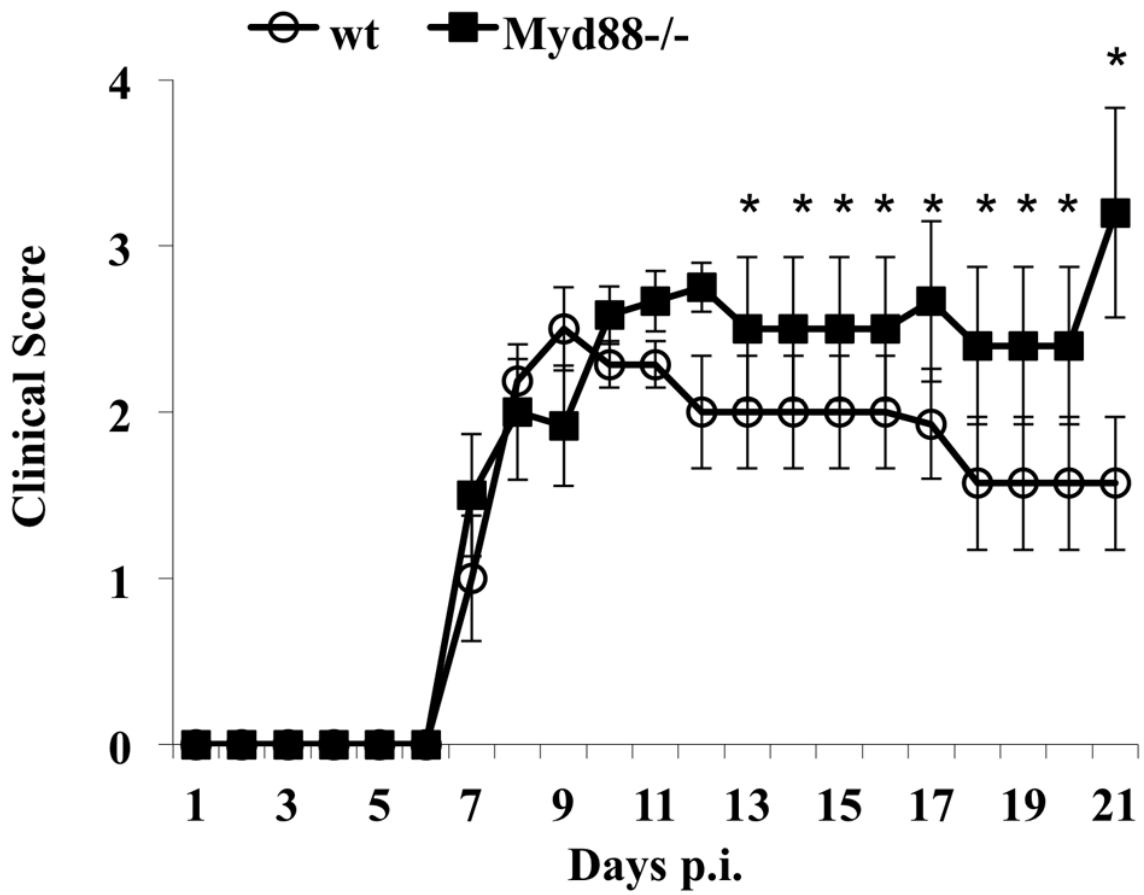


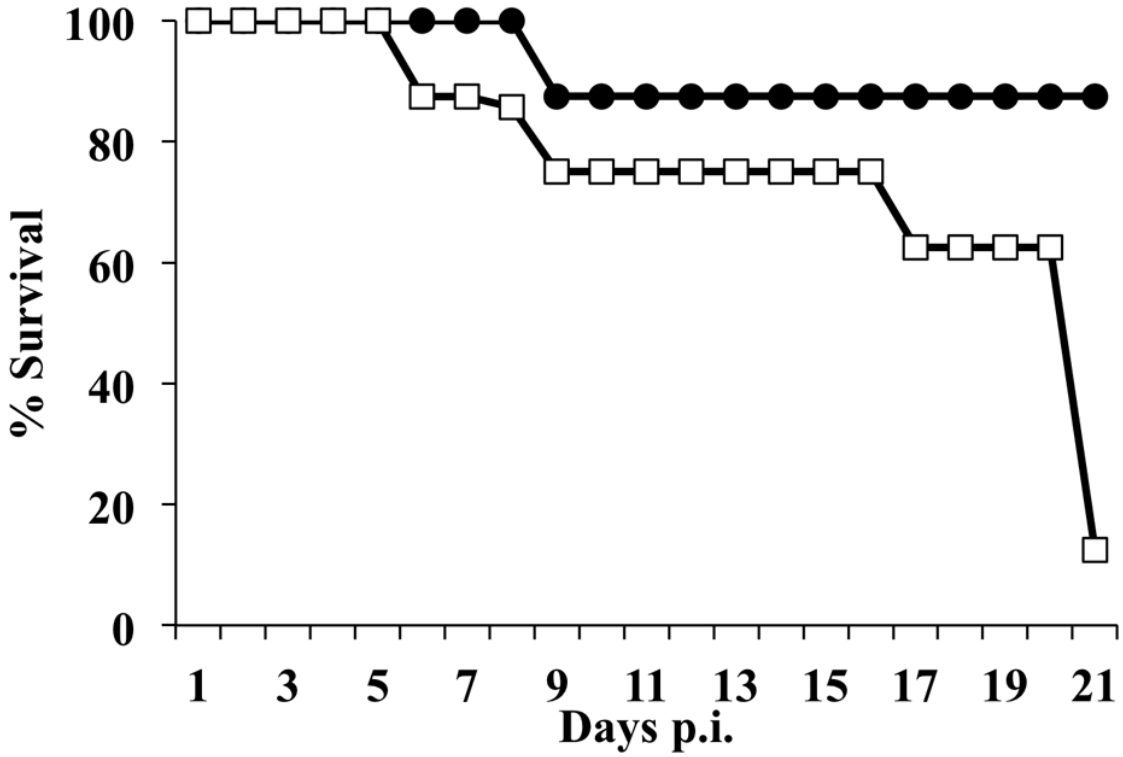

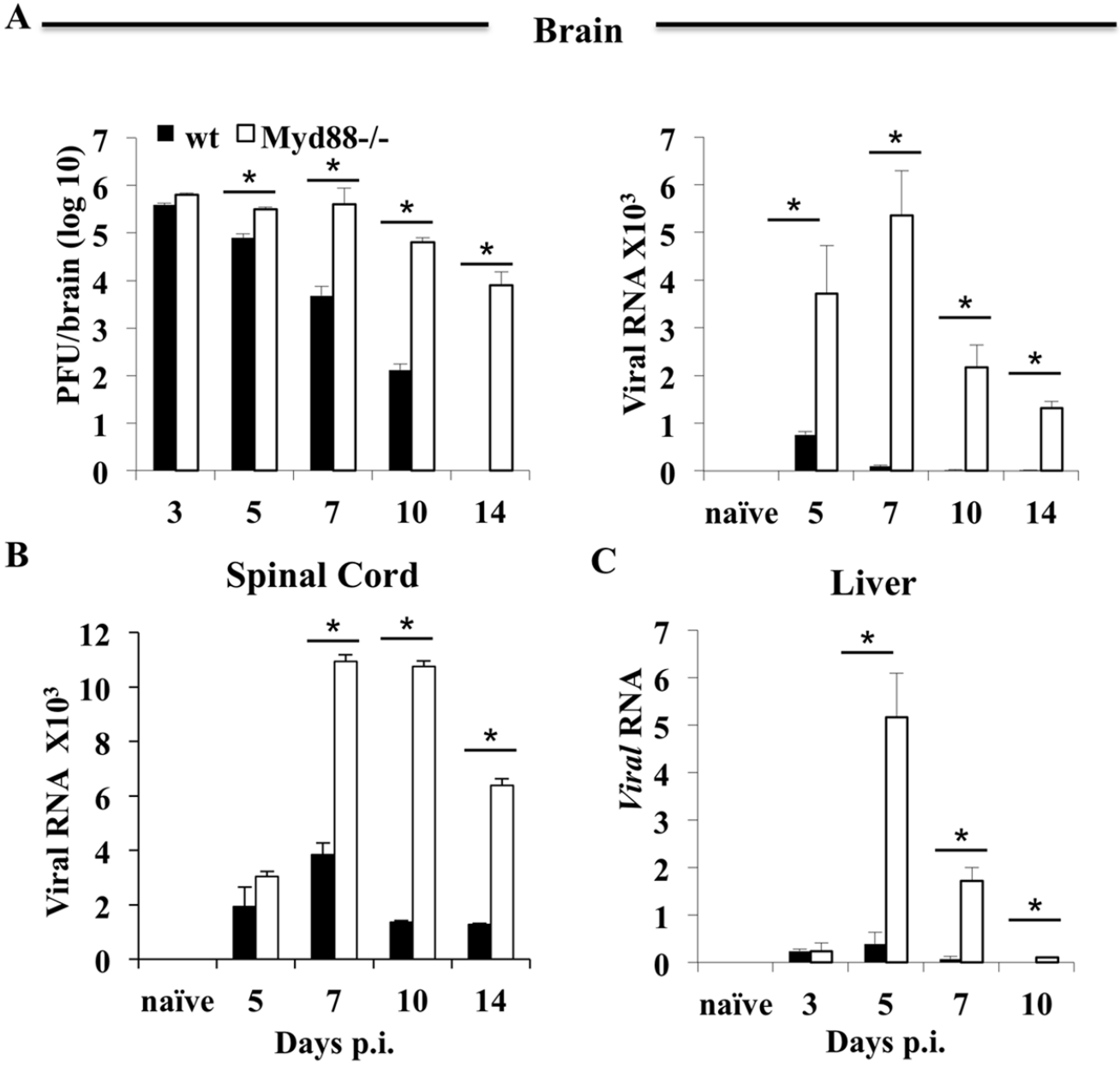

3 A

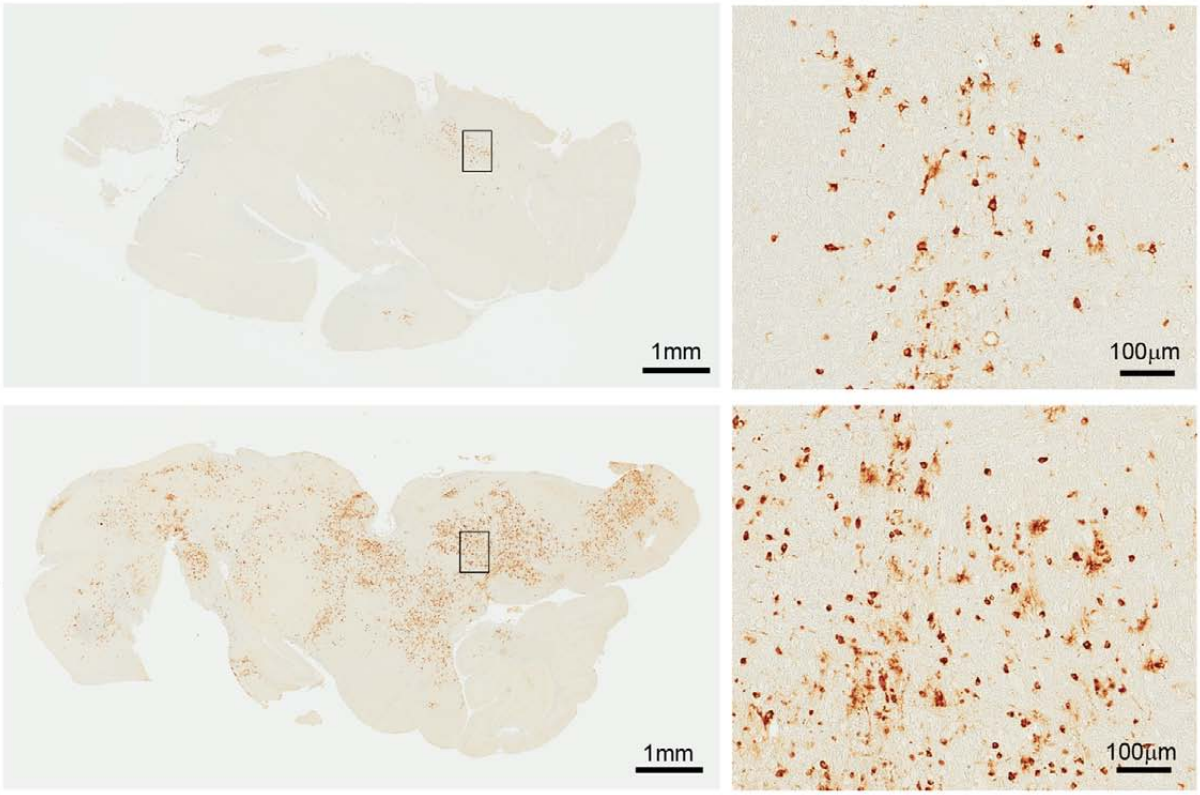


B

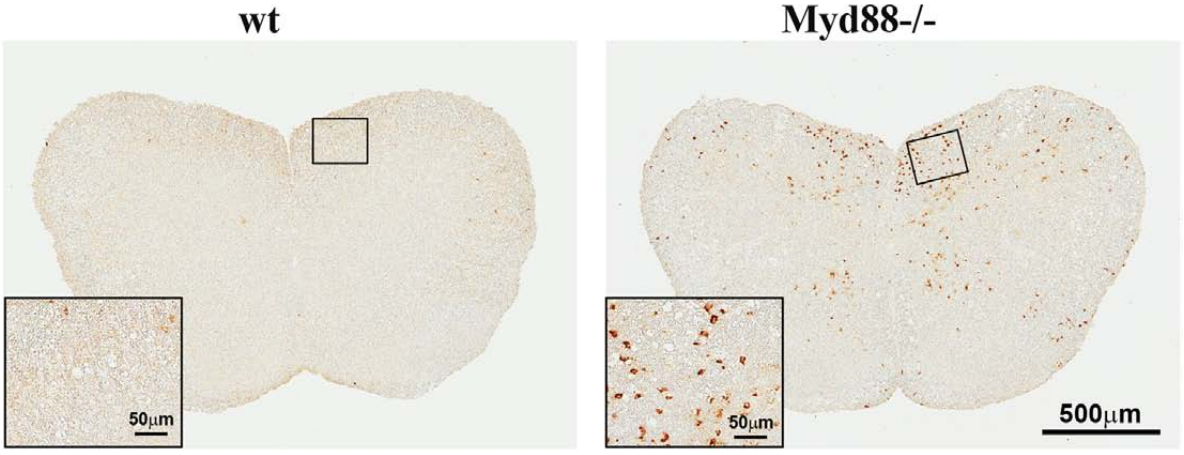

*4* **A**

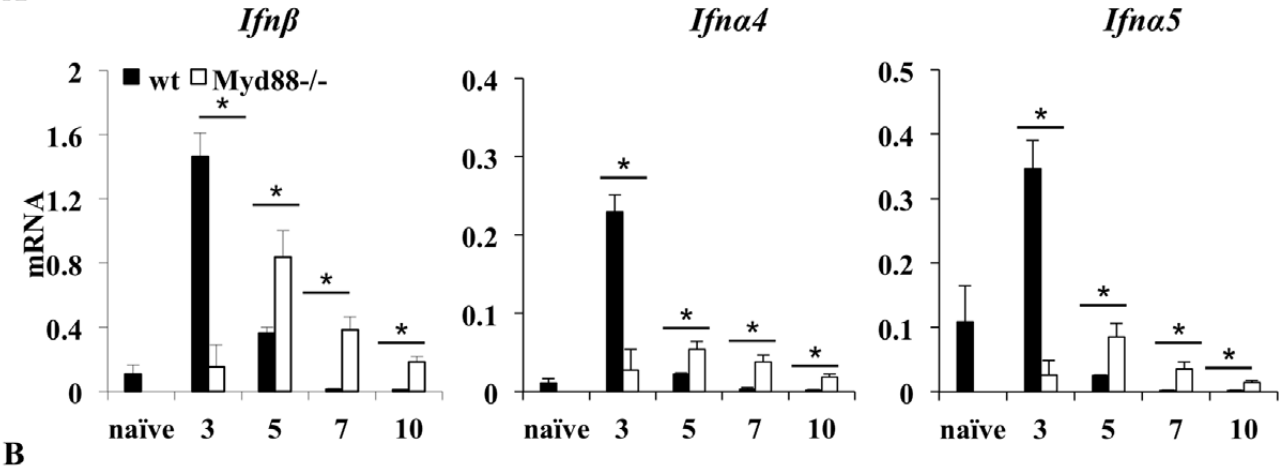


**B**

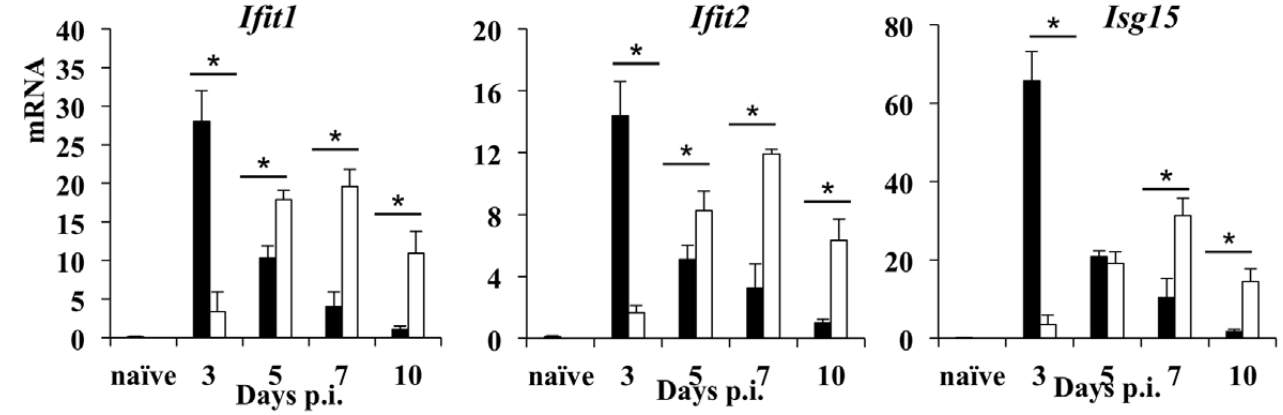

5 A

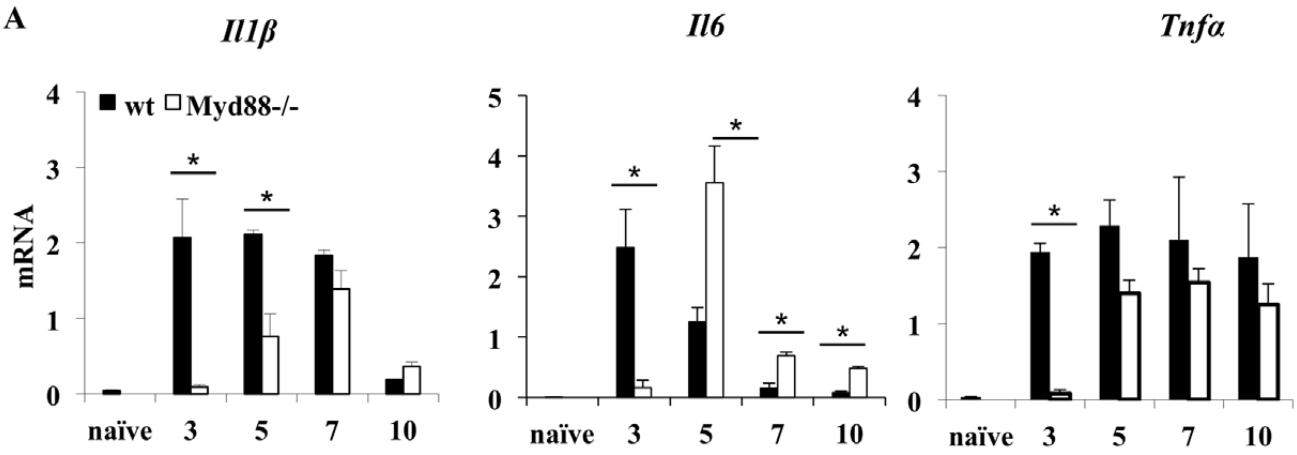


B

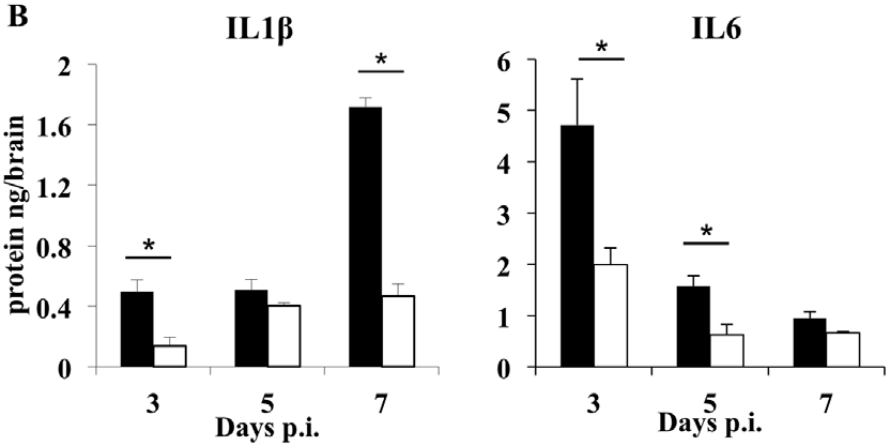

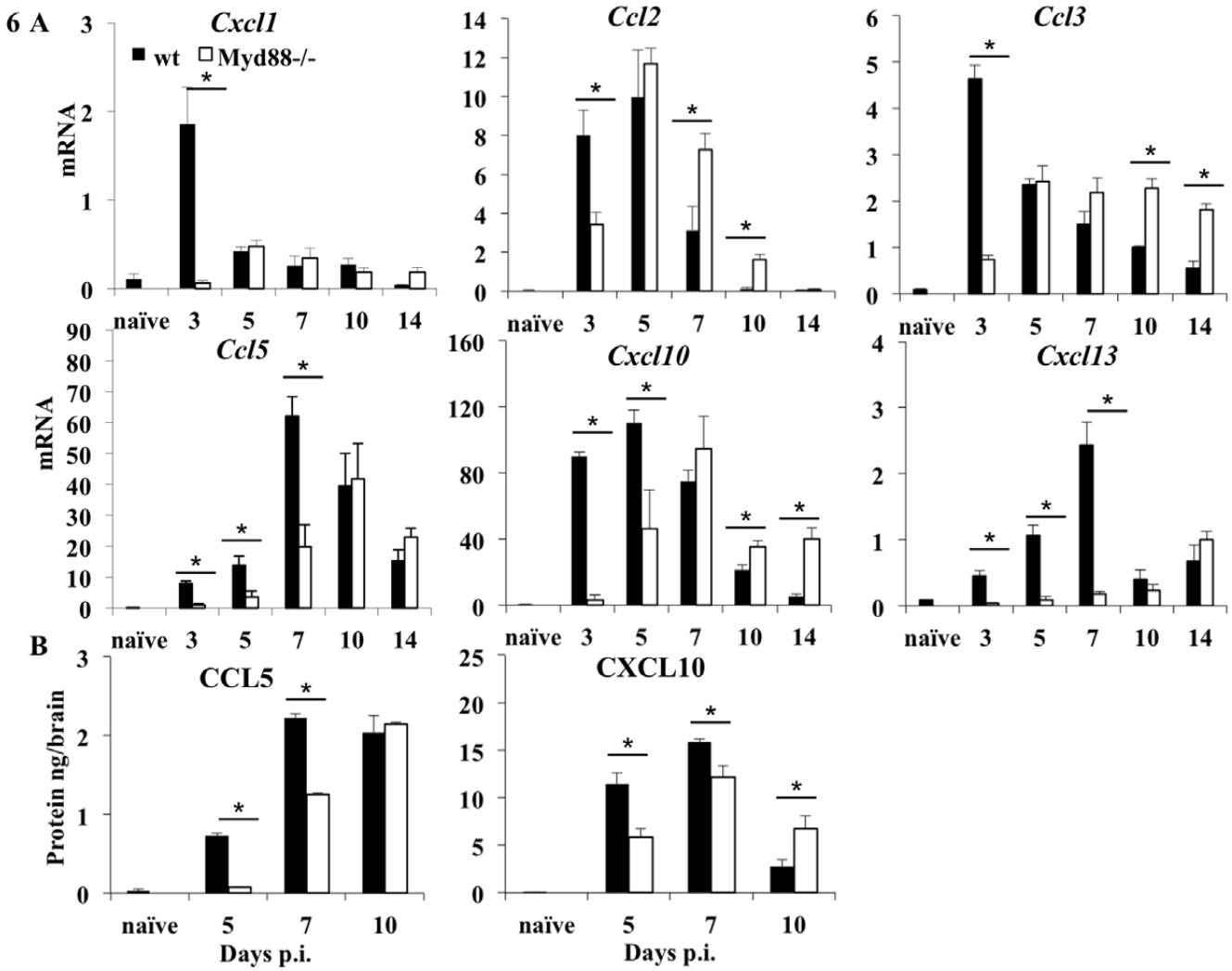

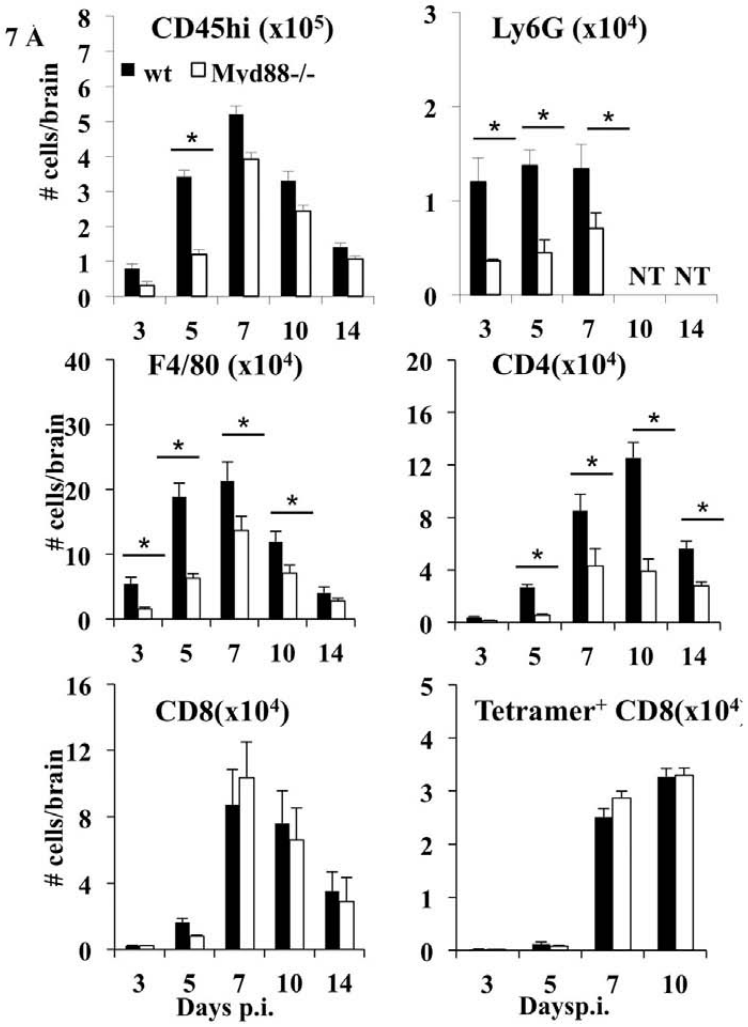


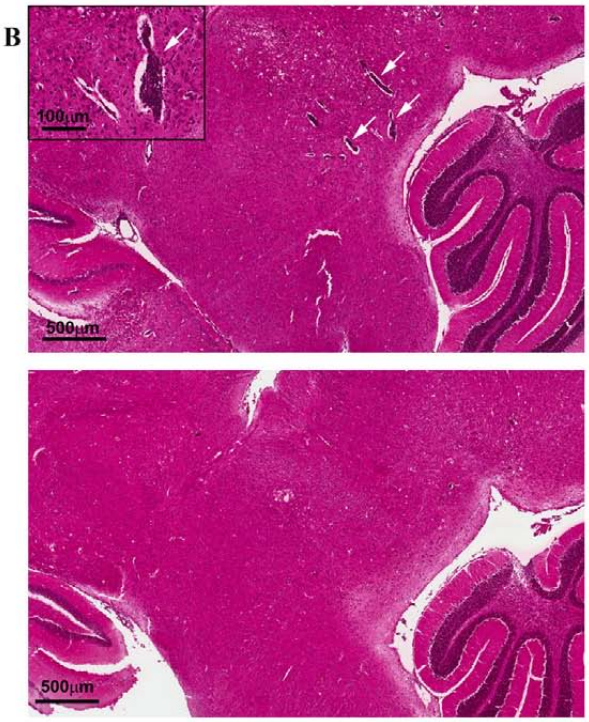

8 A

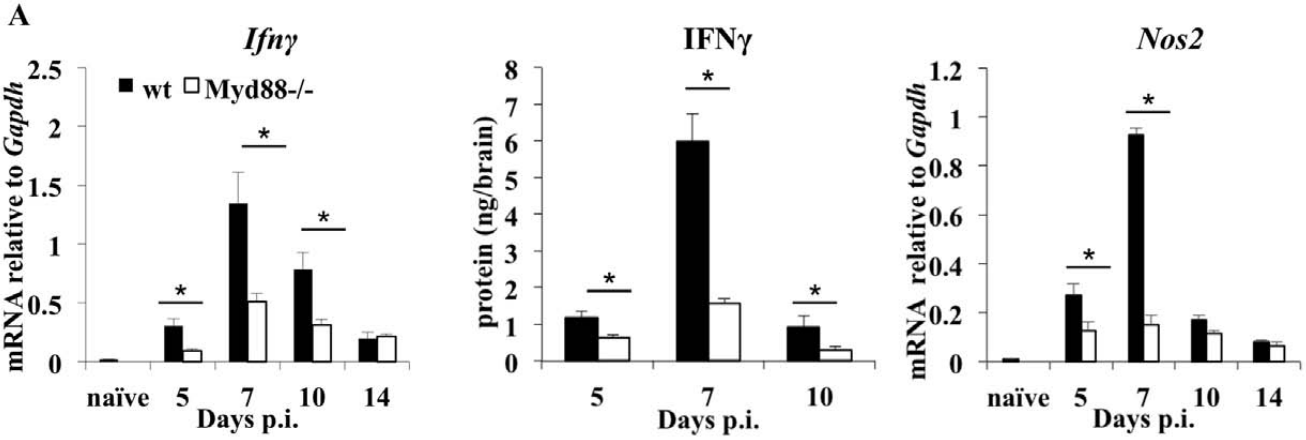


B

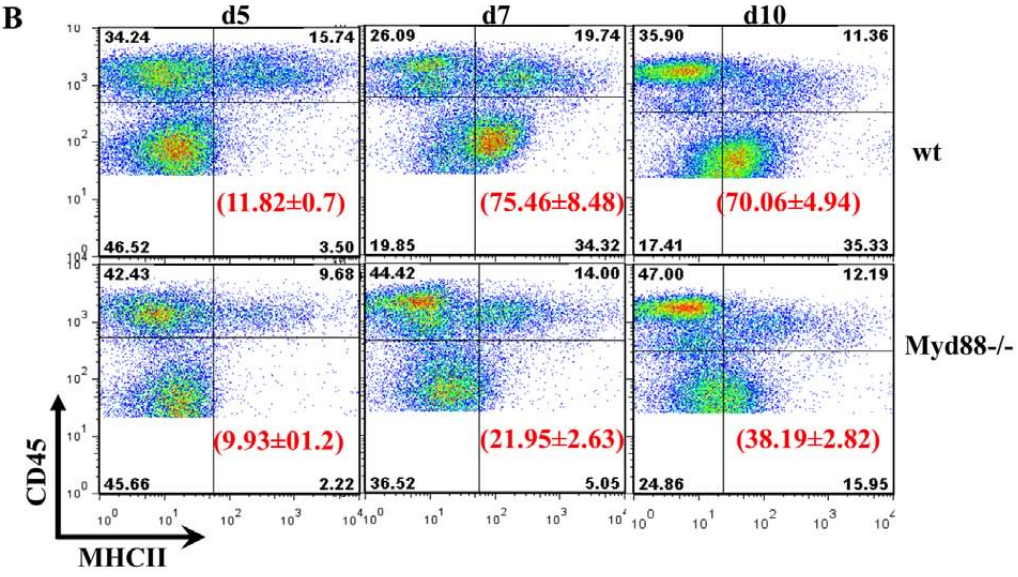

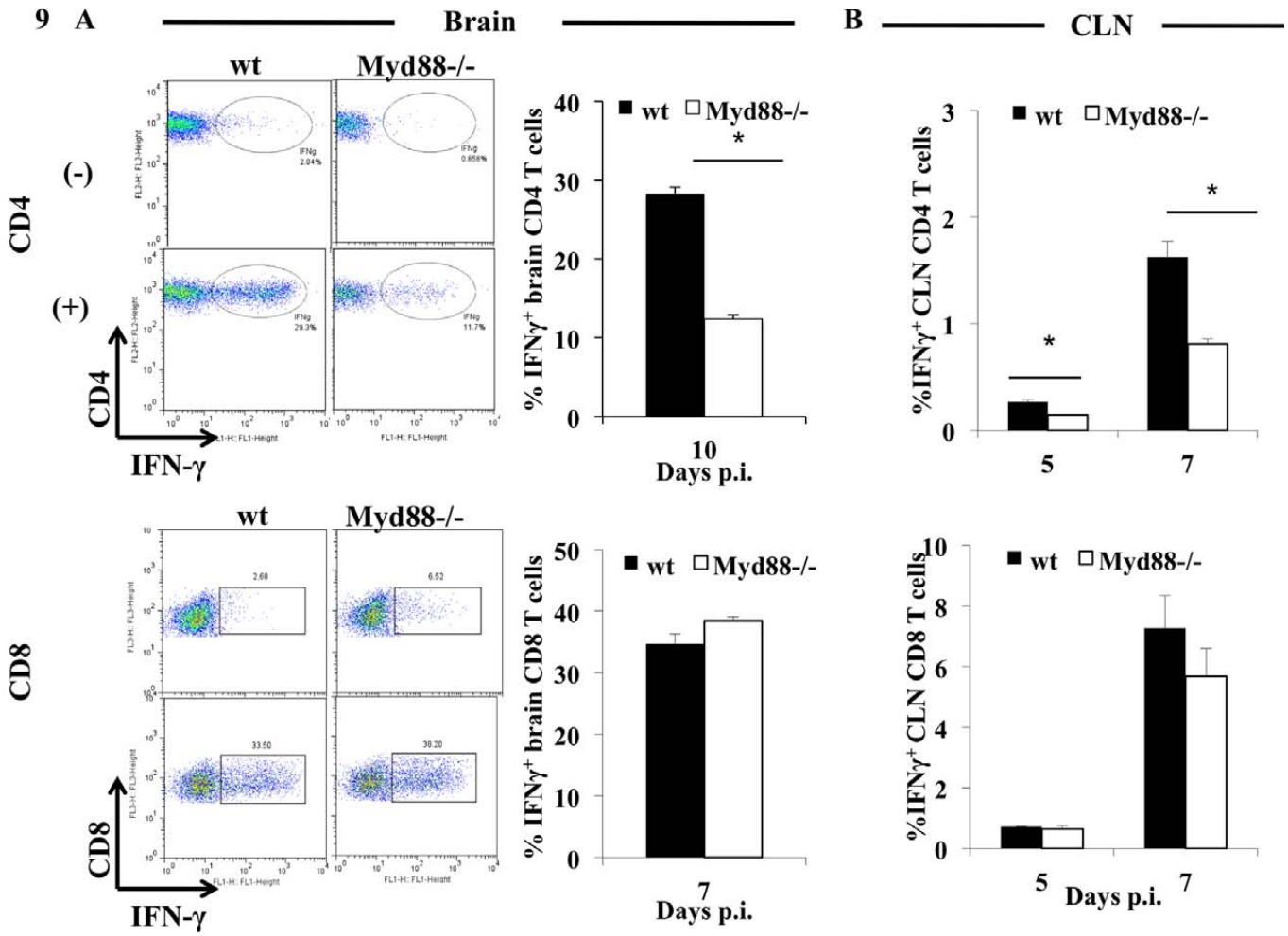




Journal of Virology